STUDIES OF LAYERED DOUBLE HYDROXIDES

THESIS

Presented to the Graduate Council of the

University of North Texas in Partial

Fulfillment of the Requirement

For the Degree of

MASTER OF SCIENCE

By

Jingxian Zhao, B.Eng, M.Eng

Denton, Texas

August, 1995

Zhao, Jingxian, Studies of Layered Double Hydroxide, Master of Science (Chemistry), August, 1995, 82 pp, 19 tables, and 39 illustrations, reference, 71 titles.

A series of layered double hydroxides (LDHs), a family of newly developed materials which being currently studied and found to have many potential use in industry, were investigated in relating to origin of life on early Earth.

In this work, I successfully intercalated some inorganic as well as organic species. Ammonium, accompanied with ferrocyanide ion, can enter the layered space. It was found there were two kind of intercalated ferrocyanide species: one is that exchanged with anions and became a part of layered double hydroxide, while the other is suggested to be related to ammonium ferrocyanide neutral species. Formaldehyde, ethanolamine and formate can also be involved into LDHs.

To improve the crystallinity, homogeneous precipitation method, which used Urea and Hexamine, was employed. The results reveal the success in the case by Urea but not in that by Hexamine. Annealing could also be used for this purpose. However, it needs to be processed in its mother liquor; no improvement on the crystallinity if the material has been washed before annealing.

ACKNOWLEDGEMENT

I would very much like to express my gratitude to my major professor Dr. Paul S. Braterman, who has introduced me to the area of research described in this study, for his consistent instruction, guidance and encouragement throughout my present work.

I wish to thank Dr. Aleixei Garbrielov, at the University of Texas at Dallas, who collected all the XRD traces in this work.

My thanks also goes to Dr. Steven Kester and Mr. David Garrett in the Department of Biology for all the kind help in the employment of electron microscopic technique.

This research was supported by the Robert A. Welch Foundation, UNT Faculty Research Funds.

TABLE OF CONTENTS

LIST OF TABLES

LIST OF ILLUSTRATIONS

CHAPTER ONE

INTRODUCTION

This work concerns some synthetic processes and basic properties of layered double hydroxides.

1.1 Properties of Layered Double Hydroxides (LDHs)

1.1.1 Introduction to Layered Double Hydroxide

The layered double hydroxides (LDH) (1) are composed of positively charged brucite-like $M(OH)_2$ layers with trivalent cations substituting for divalent cations in a certain fraction of the octahedral sites of the hydroxide sheet. The metal cations occupy the centers of octahedra whose vertices contain hydroxide ions. These octahedra are connected to each other by edge sharing to form an infinite sheet. Between the layer sheets are domains containing exchangeable anions and water molecules. These ionic layered materials also have been termed "hydrotalcite-like" compounds, by reference to the mineral hydrotalcite, $[Mg_6Al_2(OH)_{16}][CO_3]\bullet 4H_2O$, which belongs to this family or by the term "anionic clays" in mirror image resemblance to the cationic clays whose negative charge of the aluminosilicate layers are counterbalanced by intercalated cations (2).

The general formula of the LDHs is

$$[M_{1-x}^{2+}M_x^{3+}(OH)_2][X_{x/m}^{m-}]\bullet nH_2O$$

It points out the existence of two different domains: the hydroxylated layers and the

interlamellar domains. According to this formula, it is possible to imagine a wide range of such compounds by changing the nature and relative proportions of metallic cations. Moreover, such a host structure can intercalate a great number of different anionic species and strong variation in hydration state may occur.

The layer can be stacked with two layers per unit cell in hexagonal symmetry (manasseite), or with three layers per unit cell in rhombohedral symmetry (hydrotalcite), or, even, in less symmetrical arrangements (3). A schematic model is shown in Fig 1.1 (4).

1.1.2 Thermal Behavior of Layered Double Hydroxides

Generally, the thermal stability of LDHs are not as high as some metal silicates, such as clay compounds or zeolite. A layered double hydroxide loses its layered

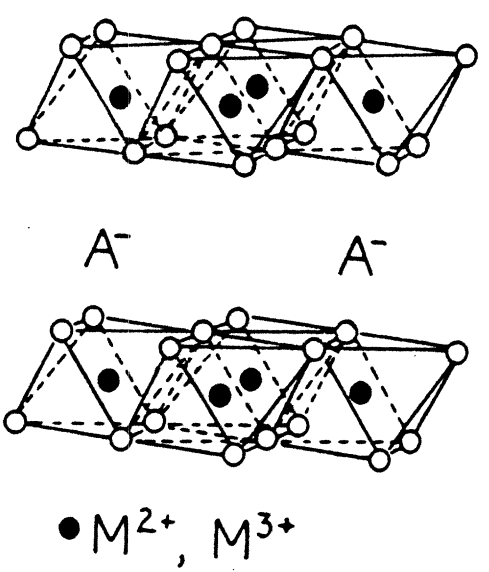

Fig 1.1 Structural model of layered double hydroxides (LDHs)

structure if the temperature is over 300°C. Thermogravimetric analysis (TGA) revealed about 30 wt% decrease when a sample was heated from 50 - 700°C (4). This weight loss is attributed to the loss of water: surface water, gallery water and structural water.

Constantino etc. (5) reported the thermal behaviors based upon TGA and XRD results of various LDH samples. It was found that at 80°C a Mg^{2+}/Al^{3+} (2/1) LDH lost about 6% of its weight which was ascribed to loosely bonded surface water. After being heated at 150°C for 2 hours it lost about 12-15 wt% of its weight. This additional loss is attributed to the water in the layered space. XRD patterns reveal that, at that stage, the LDH still remains its layered structure only with decreased interlayer distance from 0.767 nm to 0.673 nm. Nevertheless, when an LDH was heated at 250°C in N_2 it almost lost its diffraction patterns and the sample was essentially amorphous, which indicates that the degradation of LDH hydroxide was complete at 250°C. Interestingly, if the sample was heated at 250°C and cooled in air XRD patterns were mostly retained and not much change from the precursor, which indicates that the dehydrated sample can be recovered by rehydration and that the reconstruction of the LDH hydroxide upon exposure to air is a very fast and completely reversible process. Crystalline MgO appeared at 450°C and the LDH transformed to the $MgAl_2O_4$ spinel crystalline phase, along with MgO, when the temperature reached 900°C.

The mechanism for degradation is believed to involve the liberation of water through a dehydroxylation process followed by release of Cl^- from the interplan space (6-7). However, it is also possible that, in some cases, it incorporates ZnO (or MgO)

migration from the hydroxylated sheet into the inter-lamellar space, which is evidenced by ZnO crystalline appearing at 150°C, before the total collapse of the LDH structure (4). This result suggests the segregation of Zn^{2+} LDH frameworks in the dehydration process.

1.1.3 Distance Between LDH Layers

The interlamellar spacing between layers is largely determined by the size of intercalated anions as well as gallery water. Table 1.1 displays the change of the spacing with change of anions.

Table 1.1 Interlamellar spacing (Å) of ZnAlX with different anions (X) (8)

Anions	d_{003}	Anions	d_{003}	Anions	d_{003}
F^-	7.59	ClO_3^-	8.93	SO_4^{2-}	8.72
Cl^-	7.81	BrO_3^-	9.25	CrO_4^{2-}	7.86
Br^-	7.90	IO_3^-	9.72	HPO_4^-	8.56
I^-	8.48	SO_3^{2-}	7.93	MoO_4^{2-}	8.13
NO_3^-	8.81	ClO_4^-	9.05	$Cr_2O_7^{2-}$	7.85
CO_3^{2-}	7.64	ReO_4^-	9.36	$P_2O_7^{4-}$	8.89

The table clearly indicates that the layer space is strongly affected by the size of an involved anion. Moreover, the charge of an anion also plays an important role: the

higher an anion's charge the stronger of the interaction between the anion and the hydroxylated sheet and, therefore, other things being equal the smaller of layered space.

In contrary to anions, cations have not much contribution to the space distance. Table 2.2 shows the spacing change caused by different cations. Obviously these LDHs exhibit no significant changes in the spacing. This is expected as cations in an LDHs are located in the center of octahedra, which build the layered hydroxylated sheet. The change of cation's size does not greatly affect the size of the octahedra and, therefore, the spacings are expected to be comparable.

Table 2.2 Interlamellar spacing (Å) of LDHs chloride (9)

LDHs	d_{003}	LDHs	d_{003}
Mg/Al/Cl	8.13	Zn/Al/Cl	8.11
Ni/Al/Cl	8.34	Zn/Cr/Cl	7.96

Another effect which can change the spacing is the water contained in the interlamellar layers. As mentioned above, the loss of a water molecule leads to a decrease of interlayer spacing. However, this change depends upon the form of water in an LDH. As reported by Dupuis al. (10), who studied protons in $Zn_2Al(OH)_6 \cdot nH_2O$ using H^1 NMR, there were two kinds of protons, one related to OH^- in the

hydroxylated sheet (fixed phase), and the other to the water between the layered space or on the LDH surface (mobile phase). Obviously, only those waters between the layers is able to affect the spacing of LDHs. As the water molecule size is smaller than that of most anions, the change of the space distance depends upon the amount of water involved: if a sample has been dried under certain conditions (eg. 80°C) it contains a limited amount of water and the distance is largely determined by the size of anion; nevertheless, if a lot of water is involved the space between layers are somewhat expended. This change, however, is limited as LDHs could only swell by one or two water layers, unlike some smectite clays which are capable of swelling multilayers of water (9).

1.2 Applications in industry

1.2.1 Catalysis

After successful synthesis were developed in early 70's, layered double hydroxides are gathering more and more interest recently. An important application is in the area of catalysis. A considerable amount of work has been devoted to developing new catalysts (11-13), which use LDH as precursor. Unlike some clays or zeolites, which have acidic catalytic sites, LDHs mainly display base-site catalytic properties. Chemical analysis, XRD, TGA, and IR methods have been used to determine the chemical composition and structures of these materials (14,22). Further studies involving calcination, reduction and the structure of unreduced and reduced materials have shown that stable materials, which have specifically required catalytic

activities, can be prepared (23), and that their catalytic activity and structure stability are related to specific synthetic procedures.

By substituting Mg^{2+} and Al^{3+} with some catalytic active elements, such as Fe^{3+}, Co^{2+}, Ni^{3+}, Zn^{2+} and Fe^{2+}, a range of functional catalysts can be obtained. As base-centered catalysts, they are mainly employed in methanation, aldol condensation (15-16), polymerization of propiolactone and propylene oxide (17-18) etc. in which base catalytic sites are needed. These LDH materials can also be used as catalyst supports on which specific catalytic active elements are loaded. The catalysts formed by this way sometimes display multi-functional properties(19-21). For example, the active center in supports combined with that of loaded metal can form multi-catalytic-site group, which would show some properties neither of the support or loading metals would show individually. In addition, by interaction between supporting LDH and loaded metals the catalytic activity can sometimes be significantly improved.

1.2.2 Absorption of Ions and Gases

Because of their anionic exchangeability, layered double hydroxides could be used to extract some anions from a solution. Usually, Cl^- in LDHs chloride is ready to be replaced by anions having higher charge density. This property provides a chance to collect some valuable anions form a solution, or remove hazardous ones from waste water. As an example, Narita al (24-25). reported the adsorption property of aromatic sulfonate ions as well as ionic dyes by heat-treated LDH. It has also been reported (26) that gas adsorption from -196°C to room temperature using Mg/Al/$[Fe(CN)_6]$ compound show molecular sieve-like effects which depend on the size of the gas

molecule. Interestingly, no H_2 adsorption was observed while N_2, O_2, CO_2 all adsorbed.

1.2.3 Ionic Conductors

$[Zn_2Cr(OH)_6]X \bullet nH_2O$, where X = F^-, Cl^-, Br^-, I^-, CO_3^{2-}, and NO_3^-, has a relative high ability to take up water, leading to more swelling and to anion mobility (27-28). Fast proton exchange H_2O == OH^- have high proton conductivity, which is due to proton transfer between H_2O and OH^- species, in contrast with the usual involvement of H_2O and H_3O^+, in solid state conductor (28). It, thus, could be used as a conductor. Conductivities as high as 10^{-3} Ω^{-1} cm^{-1} for Zn/Cr/Cl were observed, presumably due to movement of chloride ions through channels under various humidity conditions. Other anions showed ion conductivities between 10^{-3} - 10^{-4} Ω^{-1} cm^{-1}. "Quasi-two-dimensional" electrolysis of intercalated solvated ions in layered host lattices have also been reported (29).

1.3 Application in studies of origin of life

The study about the origin of life is an interesting topic which seeks insight into the earliest chemical stages of the processes leading to life on Earth. According to the inorganic ancestor hypothesis, life started from inorganic species. The question arises, how those inorganic species in early life converted to early simple organic molecules which might have developed and evolved to modern life. The first thing we need to consider is the condition which was necessary to the conversion process. We might never be able to discover the actual conversion process and the historical conditions

involved in that process; however we could imagine those conditions and simulate the process, which will help us to understand early life.

Obviously, according to modern kinetic theories, the candidate inorganic species need to have been accumulated in some place before the conversion could happen. Moreover, some forms of energy were necessary to overcome thermodynamic barriers and transform these species to organic molecules. One can imagine that the most probable energy source was sunlight, which could produce a photochemical process. But the question of accumulating inorganic species is not so obvious. A possible way is that those inorganic species were absorbed and accumulated in some kind of solid, which acted just as the membranes of a modern cell. This hypothesis might be the starting point for the studies in the area.

If the above considerations are reasonable, a more realistic question arises, what kind of solid could play that role. Definitely, the solid must be capable of collecting some inorganic species and, more importantly, must be available on the early Earth. A layered double hydroxide might be a good candidate for the purpose as it meet both of those conditions: having large capacities of intercalating anions; available at an early stage.

As our work is a part of studies of the origin of life, we were concerned mainly the materials and processes which might relate to these topics.

REFERENCES

1. Martin, K. J., Pinnavaia, T. J. J. of Ame. Chem. Soc., **1986**, 61, 325.
2. Reichle, W. T. Solid State Ionic, **1986**, 22, 135.
3. Brindley, G. W., Kikkawa, S. Am. Mineral, **1979**, 64, 836.
4. Malki, K. E., Roy, A. D., Besse, J. P. Mat. Res. Bull, **1993**, Vol.28, 667-673.
5. Constantino, V. R. L., Pinnavaia, T. J. Inorg. Chem., **1995**, 34, 883-892.
6. Miata, S. Clays Clay Miner, **1975**, 23, 369.
7. Clearfield A., Kieke, M., Kwan, J., Colon, J. L., Wang, R. C. J. Inclusion Phenom. Mol. Recognit. Chem., **1991**, 11, 361.
8. Malki, K. E., Guonano, C., Forano, A., Roy, A. D., Besse, J. P. Mat. Sci. Forum, **1992**, Vol.91-93, 171-176
9. Carrodo, K. A., Kostapapas, A. Solid State Ionics, **1988**, 26, 77-86.
10. Dupuis, J., Battut, J, P., Fawal, Z., Hajjimohamad, H. Solid State ionics, **1990**, 42, 251-255.
11. Chibwe, K., Valim, J. B., Jones, W. Abstracts of papers of the American Chemical Society, **1989**, vol.198, 20
12. Perezbernal M. E., Ruanocasero, R., Pinnavaia, T. J. Cat. Lett., **1991**, vol.11, 55-62.
13. Narita, E., Kaviratna, P., Pinnavaia, T. J. Chem. Lett., **1991**, 5, 805-808
14. Labajos, F. M., Rives, v., Ulibarri, M. A. Spectrosc. Lett., **1991**, vol.24, 499-508.
15. Reichle, W. T. J. Cat., **1985**, 94, 547.

16. Reichle, W. T. Solid State Ionics, **1986**, 22, 135

17. Kokjiya, S. Sato, T., Nakayama, T., Yamashita, S., Makromol. Chem. Rapid Comm., **1981**, 2, 231

18. Nakatsuka, H., Kawasaki, S., Yamashita, S., Kokjiya, S. Bull. Chem. Soc. Japan, **1979**, 52, 244a.

19. Pinnavaia, T. J., Rameswaran, M., Dimotakis, E. D., Giannelis, E. P., Rightor, E. G. Faraday Discussions of the Chemical Society, **1989**, 87, 227-237.

20. Martin, K. J., Pinnavaia, T. J. J. Ame. Chem. Soc., **1986**, 108, 541-542.

21. Rameswaran, M., Pinnavaia, T. J., Abstracts of Papers of the American Chemical Society, **1988**, 196, 55

22. Kruissink, E. C., Van Reijden, L. L. J. Chem. Soc. Farad. Trans., **1981**, I 77, 649.

23. Alzamora, L. E., Ross, J. R. H., Kruissink, E. C., Van Reijen. J. of Chem. Soc. Farad. Trans., **1981**, I 77, 665.

24. Narita, E., Yamagishi, T., Tonai, T. Nippon Kagaku Kaishi, **1992**, 3, 291-296.

25. Narita, E., Yamagishi, T., Suzuki, K. Nippon Kagaku Kaishi, **1992**, 6, 676-679.

26. Miyata, S., Hirose, T. Clays Clay Miner, **1978**, 26, 441

27. Lai, M., Howe, A. T. J. solid state chem., **1981**, 39, 337.

28. Lai, M., Howe, A. T. J. Chem. Soc. Chem. Comm., **1980**, 737.

29. Schollhorn, R., Otto, B. J. Chem. Soc. Chem. Comm. **1986**, 1222.

30. Shaw, B. R., Deng, Y. P., Strillacci, F. E., Carrado, K. A., Fessehaie, M. G. J. Electrochem. Soc. **1990**, vol.137, 3136-3143.

31. Braterman, P. S. A Proposal to NASA, **1994**.

32. Robbins, E. I., Iberall, Geomicrobiology Journal, **1991**, vol.9, 51-66.

33. Schollhorn, R., Otto, B. J. Chem. Soc. Chem. Comm., **1986**, 1222.

34. Chibwe, K., Jones, W. J. Chem. Soc. Chem. Comm., 1989, 926-927.

35. Kwon, T., Tsigdinos, G. A., Pinnavaia, T. J. J. Am. Chem. Soc., **1988**, vol.10, 3653-3654.

36. Martin, K. J., Pinnavaia, T. J. J. Am. Chem. Soc., **1986**, vol.108, 541-542.

37. Wang, J. D., Tian, Y., Clearfield, A. Abstracts of papers of the American Chemical Society, **1992**, vol.203, 785.

38. Park, I. Y. J. Chem. Soc. Dolton, **1990**, 3071.

39. Grosso, R. P., Suib, S. L., Weber, R. S., Schubert, P. F. Chemistry of Material, **1992**, vol.4, 922-928.

40. Meyn, M., Bebeke, K., Lagaly, G. Inorg. Chem., **1990**, vol.29, 5201-5207.

CHAPTER TWO

TECHNIQUES EMPLOYED

2.1 Fourier Transform Infrared Spectroscopy (FTIR)

FTIR is a commonly employed method of determining the chemical groups in either crystalline or amorphous phases. Each chemical group absorbs characteristic frequencies of infrared radiation uniquely. Thus an infrared spectrum fingerprints the identifiable chemical groups in the unknown.

FTIR is widely employed for organic characterization. Its application in inorganic chemistry, though less widespread, has also been established(3-7). Inorganic anions such as carbonate, sulfate, ferrocyanide, ferricyanide, silicate, nitrate, and also the ammonium cation show their characteristic vibrational bands in the mid-IR region. However, unlike organic species, their exact absorbing wavelengths are affected by the cations they are attached to; peak shifts are normally observed when the cation is changed. This because that vibrational frequencies are influenced by the reduced mass (μ) involved as illustrated in the following equation:

$$\nu = 1/(2\pi) * \sqrt{k/\mu}$$

Another special feature with inorganic compounds or minerals is that their infrared spectra are affected by crystallinity. Because of intermolecular interaction, the symmetry of a molecule is generally lower in a crystalline state than in the gaseous (isolated) state. This change in symmetry may split the degenerate vibrations and

activate IR-inactive vibrations. For example, the symmetry for isolated CO_3^{2-} is D_{3h}. In calcite crystal the symmetry is D_3 and in aragonite the symmetry is lowered to C_s. The four characteristic vibrations for calcite and aragonite are listed in Table 2.1. Evidently, the IR-inactive ν1 in calcite (not net dipole moment change) is activate in aragonite; also the ν3 and ν4 vibrations are split in aragonite crystals.

The FTIR system employed in our experiments was a Perkin-Elmer 7600 with computer interface.

Table 2.1 Vibrational Frequencies of Planar CO_3^{2-} in the Crystalline State (cm^{-1}) (17)

structure	ν1	ν2	ν3	ν4
Calcite	inactive	879	1429-1492	706
Aragonite	1080	866	1504, 1492	711, 706

2.2 Scanning Electron Microscopy (SEM)

Similar to optical microscopes, the electron microscope serve to magnify minute objects normally invisible to the naked eye. However, microscopy uses an electron beam instead of a light beam or ultraviolet rays as a means of specimen illumination.

The scanning microscopy is one of the most versatile instruments available for the examination of objects. The primary reason for its usefulness is the high resolution which can be obtained when bulk objects are examined; values of the order of 2.5 nm

are quoted for advanced research instruments (20). Another important feature of the SEM is the three-dimensional appearance of the specimen image, which is a direct result of the large depth of focus. Moreover. it is possible to use bulk specimens with the scanning electron microscope, but not with the transmission electron microscope.

The operational principle of the scanning electron microscope is illustrated in Fig 2.1. A finely focused electron probe is made to scan the specimen surface, with the result that secondary and backscattered electrons etc. are emitted from the specimen surface. These signals are then detected and fed to a synchronously scanned CRT as an intensity modulating signal, thus displaying a specimen image on the CRT screen. The CRT raster width divided by the electron probe scanning width gives the image magnification.

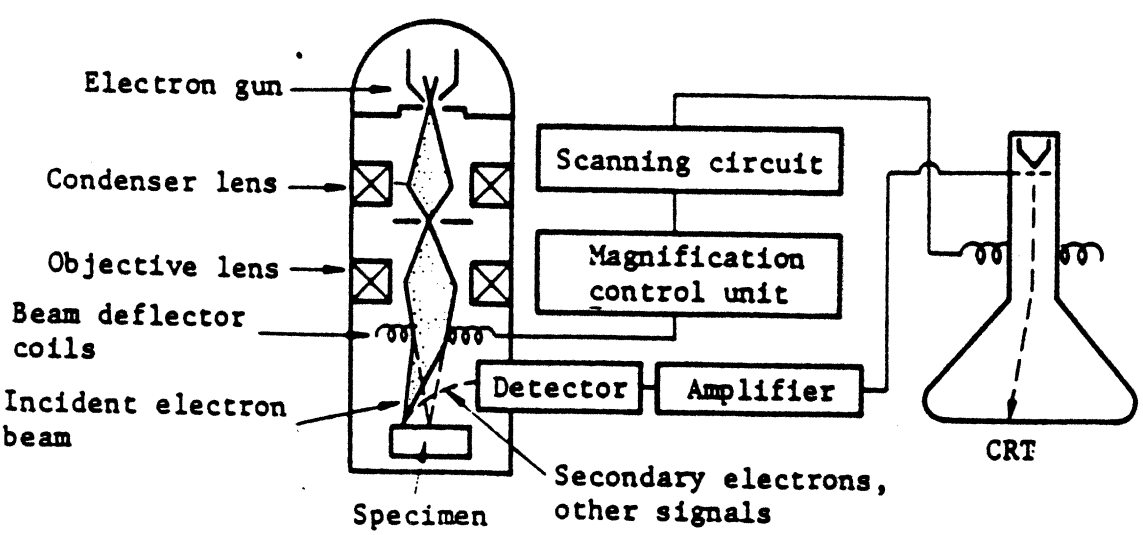

Fig 2.1 The operating principle of SEM (22).

2.3 X-Ray Diffraction (XRD)

The X-ray date reported here were obtained by Dr. Alexei Gabrielov at the University of Texas at Dallas using a Scintag powder diffractometer. CaF_2 was used in many cases as an internal standard.

X-ray diffraction provides a convenient and practical means for the qualitative identification of crystalline compounds. This application is based upon the fact that an X-ray diffraction pattern is unique for each crystalline substance. Thus, if an exact match can be found between the pattern of an unknown and an authentic sample, chemical or structural identity can be assumed. In addition, diffraction data sometimes yield quantitative information concerning a crystalline compound in mixture. The method may provide data that are difficult or impossible to obtain by other means as, for example, the percentage of graphite in a graphite/charcoal mixture. More significantly, if a reference is quantitatively included, this method could also reveal information abort the possible conformation of species in a crystal after some physical or chemical treatment.

XRD is based on Bragg's law (18)

$$n\lambda = 2d * \sin\theta$$

where λ is the wavelength of the x-ray beam, d is the interplanar distance of a crystal, θ is the angle between the incident x-ray and the reflecting crystal plane, and n is an integer representing the order of reflection (in practice n is taken to be 1). Bragg's law indicates that x-rays are reflected from the crystal only if the angle of incidence satisfies the condition that $\sin\theta = n\lambda/2d$.

REFERENCES

1. Kandall, D. N. Applied Infrared Spectroscopy; Chapman &. Hall Ltd. London, **1966**.
2. Durig, J. R. in Chemical, Biological and Industrial Application of Infrared Spectroscopy; John Wiley &. Sons, New York, **1985**.
3. Clark, R. J. H., Huster, R. E. in Spectroscopy of Inorganic-based Materials; Vol.14, John Wiley &. Sons, New York, **1987**.
4. Henning, O. in The Infrared Spectrum of Minerals; Farmer, V. C. Ed.; Mineralogical Society: London, **1974**, Chapter 19.
5. Sakurai, T., Sato, T., Yoshinaga, A. Proc. 5th Int. Symp. Chem. Cem., Tokyo, **1968**, Vol.1, pp 300-321.
6. Ortego, J. D., Jackson, S., Yu, G., McWhinney, H., Cocke, D. L. J. Environ. Sci. Health, **1989**, A24(6).
7. Mollah, M. Y. A., Tsai, Y. N., Hess, T. R., Cocke, D. L. J. Hazardous Materials, **1992**, 30(3), 273-283.
8. Farraro, J. R., Rein, A. J. in Fourier Transform Infrared Spectroscopy--Application to Chemical Systems; Ferraro, J. R., Basile, L. J., Eds., Academic Press: Orlando, Florida, **1985**, Vol.4, Chapter 6.
9. Cullity, B. D., in Elements of X-ray Diffraction; Addison-Weiley ed., Massachusetts, **1987**, pp 284.

10. Kannan, S., Swamy, C. S. J. Mat. Sci. Let., **1992**, 11, 1585-1587.

11. Zhao, B. PhD Dissertation, University of North Texas, **1993**

12. Skoog, D. A. Principle of Instrumental Analysis; 3rd ed., Saunders College: Philadelphia, **1985**, pp 257-258.

13. Powder Diffraction file-Inorganic phases, International Center for Diffraction Data: Swartmore. PA. **1983**.

14. Fraser, D. J. J., Griffiths, P. R. Appl. Spectrosc. **1990**, 44(2), 193-199.

15. Van Every, K. W., Griffiths, P. R. Appl. Spectrosc. **1991**, 45(3), 347-359.

16. Leyden, D. E., Shreedhara Murthy, R. S. Spectroscopy, **1986**, 2, 28-36.

17. Nakamoto, K. Infrared and Raman Spectra of Inorganic and Coordination Compounds, 4th ed., John Wiley &. Sons, New York, **1986**, pp 86-88, 124.

18. Lipson, H., Steeple, H. Interpretation of X-ray Powder diffraction Patterns, St. Martin's Press, New York, **1970**, pp 32.

19. Bentley, F. F., Smithson, S. D., Rozek, A. L. Infrared Spectra and Characteristic Frequencies 700-300 cm^{-1}, Interscience Publishers, New York, **1968**.

20. Broers, A. N. SEM/1974, IIT research Institute: Chicago, **1974**.

21. Fryer, J. R. The Chemical Application of Transmission Electron Microscopy, Academic Press: London, **1979**.

22. Introduction to JSM-T 300 Scanning Microscope, JEOL LTD / JEOL Technics Ltd, Tokyo, Japan, **1980**.

23. Lee, Y. Thesis for Master Degree, Univ. North Texas, **1991**.

CHAPTER THREE

RESULTS WITH LAYERED DOUBLE HYDROXIDES

3.1 Materials Used

All the chemicals, along with their grade and suppliers, used in the present work were listed in Table 3.1. These materials were in general used without further purification. Water was ultra pure deionized water (Millipore, 18 MΩ) or high purity water (purchased from Baxter Healthcare Corp.) which, in some cases, was degassed by boiling for half an hour and cooled to ambient temperature under N_2.

3.2 Experimental

3.2.1 Synthesis of LDHs

Most LDHs, unless specified, were prepared by the procedure described as below.

The general formula for the LDHs studied here is $[M_2^{2+}M^{3+}(OH)_6]X_{1/n}^{n-}.mH_2O$, where M^{2+} = Mg^{2+}, Zn^{2+}, M^{3+} = Al^{3+}, Fe^{3+}, and X^{n-} = Cl^-, CO_3^{2-}, SO_4^{2-}, $Fe[(CN)_6]^{4-}$, S^{2-}, $Fe[(CN)_6]^{3-}$, $HCOO^-$.

By the formula described the M^{2+}/M^{3+} ratio is 2:1. This ratio was reached by using extra M^{2+} (M^{2+}/M^{3+} = 3) combined with titration, which stopped at twice the volume needed to precipitates M^{3+} as $M(OH)_3$ (the first equivalence point in the titration).

In the preparations of LDHs, all salts of M^{3+} ions were 0.1 M concentration and salts of M^{2+} ions were of 0.3 M solution. The concentration of related anions was

Name	Grade	Supplier
$AlCl_3 \cdot 6H_2O$	99 %	Aldrich
Ethanolamine	Regent	Aldrich
$FeCl_3 \cdot 6H_2O$	Analytic Regent	Mallinckrodt
H_2O_2	3 %, Regent	J.T.Baker
HCOH	36.5-38.0 %	EM Science
HCOOK	99 %	Aldrich
Hexamine	Sublimed	Aldrich
K_2CO_3	Regent	Spectrum Chem. Mfg
$K_3[Fe(CN)_6]$	Regent	J.T.Baker
$K_4[Fe(CN)_6]$	99 %	Aldrich
$MgCl_2 \cdot 6H_2O$	99 %	Aldrich
Na_2S	Regent	Aldrich
Na_2SO_4	Regent	Spectrum Chem. Mfg
NaCl	Regent	J.T.Baker
NaOH	50 % Solution	Fisher Scientific
$(NH4)_4[Fe(CN)_6]$	Regent	Aldrich
Urea	ACS Grade	Mallinckrodt
$ZnCl_2$	98 %	Aldrich

Table 3.1 Chemicals used for LDHs

1.0 M, except for CO_3^{2-} and SO_4^{2-} which were 0.5 M. Typically 200 ml of M^{2+}/M^{3+} solution, with those providing expected anions, was magnetically stirred in a 500 ml three-neck round bottom flask. A burette was positioned to deliver 2 M NaOH solution, which was added slowly, and pH was monitored during titration. The total volume of NaOH solution, prepared by distillation of Fisher 50% NaOH (low in carbonate), to make $M^{2+}/M^{3+} = 2$ was twice that for the first equivalence point.

The end pH typically was about 10. Precipitates appeared in different colors according to the different cations or anions used. The resulted mixture was refluxed overnight, stirred by magnetic stirrer. Afterwards, it was centrifuged, washed three times with water and dried at ambient temperature, in a 2 L nitrogen flushed glass desiccator protected where indicated.

3.2.2 Anion Exchange

$M_2^{2+}M^{3+}(OH)_6X_{1/n}^{n-}$ ($M^{2+} = Mg^{2+}$; $M^{3+} = Al^{3+}$, Fe^{3+}; $X^{n-} = Cl^-$, CO_3^{2-}) was used to exchange with various anions, such as $[Fe(CN)_6]^{4-}$, SO_4^{2-}, S^{2-}, etc. This reaction proceeded at ambient temperature. Unless specified, typically 0.5 gram of LDH in 20 ml water was magnetically stirred with selected anions (1.0 M) for overnight. The resulted mixture was washed with water three times and dried at ambient temperature.

3.2.3 $Mg_2Al(OH)_6(CO_3)_{1/2}$ exchanged with $K_4[Fe(CN)_6]$, $(NH_4)_4[Fe(CN)_6]$

The procedures were similar to general anion-exchange except that the flask used was wrapped with aluminum foil to protect it from light. The exchanging process was continued as long as necessary. The extent of exchanging was monitored by FTIR.

3.2.4 Heating of $Mg_2Al(OH)_6(CO_3)_{1/2}$ after exchange with $(NH_4)_4[Fe(CN)_6]$

0.5g of an exchanged sample in 20 ml water was transferred into a 50 ml round bottom flask, which was wrapped with aluminum foil and partially immersed in an oil bath. The bath was then heated slowly to 95°C and the mixture was stirred magnetically for a week at that temperature.

3.2.5 Homogenous Precipitation by Urea and Hexamine

The major procedures were similar to those described in LDHs synthesis. However, instead of NaOH, urea or hexamine, $N_4(CH_2)_6$, was employed. The urea (or hexamine) solution was added slowly after the $AlCl_3$ and $MgCl_2$ (or $ZnCl_3$) solution had been heated to 90°C. The mixture was then, stirred at 95°C for 5 hrs and, afterwards, refluxed fairly gently overnight. Precipitates started to show after about two hours stirring at 95°C and, apparently, ended with far less amount than that obtained by non-homogenous precipitation.

3.2.6 Oxidation of $M_2^{2+}M^{3+}(OH)_6S_{1/2}$ (S-formed LDHs)

The S-formed LDHs were prepared by using related Cl^--formed LDHs (Cl^- as anion) exchanged with Na_2S. The S^{2-}-formed LDH was then stirred at ambient temperature with 3% H_2O_2 for several days. The suspension was washed with water three times and dried at room temperature.

3.2.7 Annealing of LDHs

A selected LDH sample, 1.0g in 15 ml water, was transferred into a teflon digestion bomb (25.4 mm in diameter, 95.0 mm in height, supplied by Parr Instrument Company), which is protected by stainless steel jacket. It was then set vertically in an

oven for 1 week, with the temperature being 140°C. Afterwards, the sample was washed with water and dried at ambient temperature.

3.2.8 Preparation of FTIR Samples

The selected sample was mixed and ground with pre-dried KBr powder. The mixture so formed was then physically pressed into a thin disk (7mm in diameter), by using a KBr "Quick Press" supplied by Perkin Elmer Corporation (Fig 3.1).

3.3 Results and Discussions

3.3.1 Ion exchange of LDHs with Ferrocyanide salts

3.3.1.1 $Mg_2Al(OH)_6Cl$ with Ferrocyanide salts

Ferrocyanide or ferricyanide-formed LDHs can be easily obtained by exchanging related Cl-formed LDHs with $M_4^+[Fe(CN)_6]$ ($M^+ = NH_4^+$, K^+). Both Potassium and Ammonium Ferrocyanide could be used for intercalation. However, there are some differences between these two cases. Figs 3.2-3.3 depict the FTIR spectra for the samples exchanged 1 and 8 days by Potassium ferrocyanide, while Figs 3.4-3.6 demonstrated those exchanged 1, 5 and 8 days by Ammonium ferrocyanide. The peaks in the figures around 2025 cm^{-1} (peak a) and 2083 cm^{-1} (peak b) are assigned to the stretching vibration between C and N (1-2,6). Both peaks appeared in the case of ammonium ferrocyanide (Fig 3.5-3.6), but only the peak at 2025 cm^{-1} appeared in that of potassium ferrocyanide (Fig 3.3). By comparing these figures we can see that after 1 day of exchange both cases displayed similar behavior: only the peak at 2025 cm^{-1} appeared. However, in case of $(NH_4)_4Fe[(CN)_6]$, as time passed, the peak at 2083 cm^{-1} appeared and gradually became predominant. This result suggests that there might be

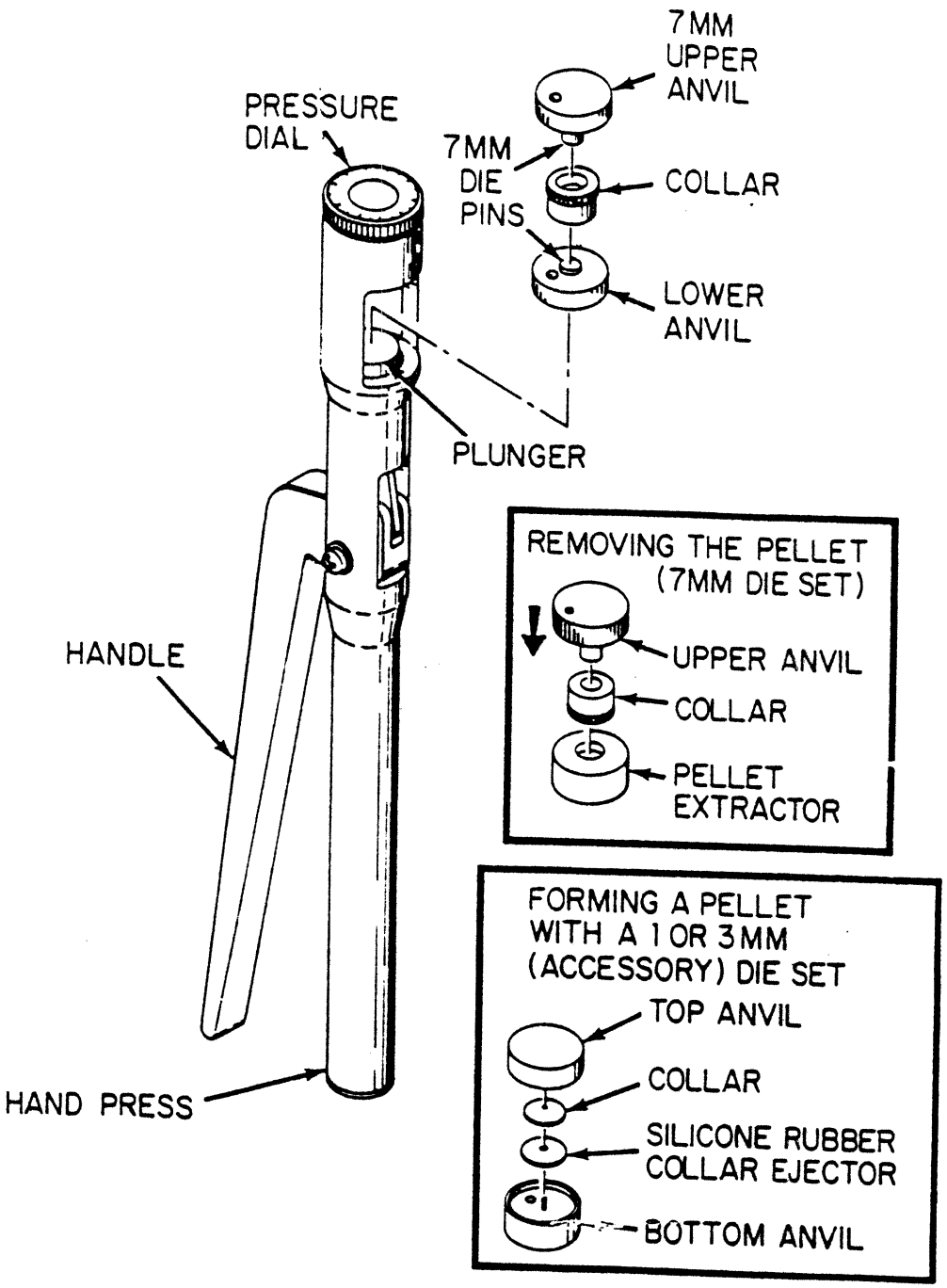

Fig 3.1 Kbr "Quick Press" with die sets

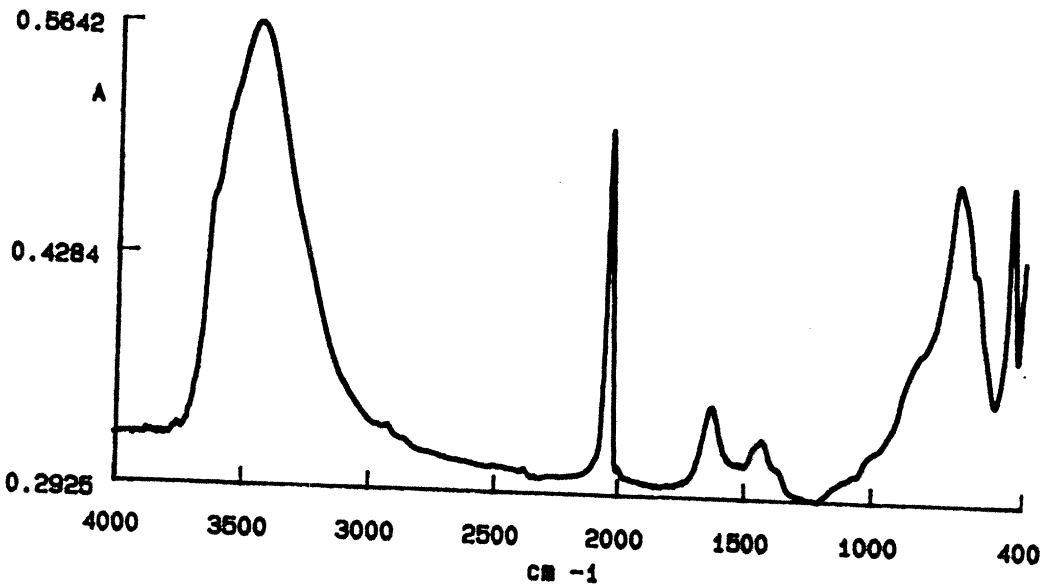

Fig 3.2 FTIR Spectrum of $Mg_2Al(OH)_6[Fe(CN)_6]_{1/4}$, by exchange of $Mg_2Al(OH)_6Cl$ with $K_4[Fe(CN)_6]$ for 1 day.

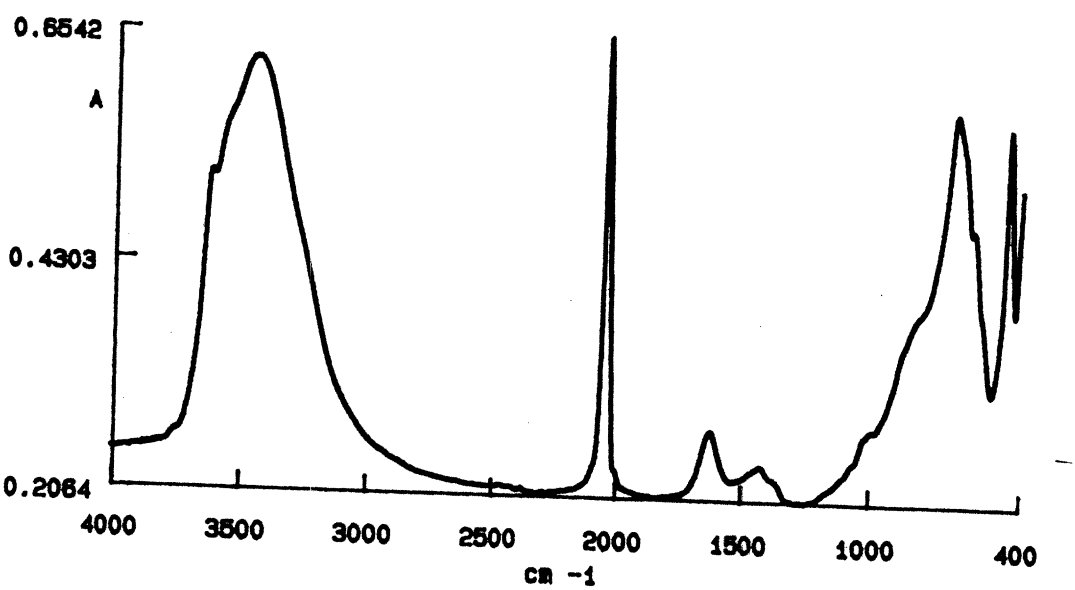

Fig 3.3 FTIR Spectrum of $Mg_2Al(OH)_6[Fe(CN)_6]_{1/4}$ by exchange of $Mg_2Al(OH)_6Cl$ with $K_4[Fe(CN)_6]$ for 8 days.

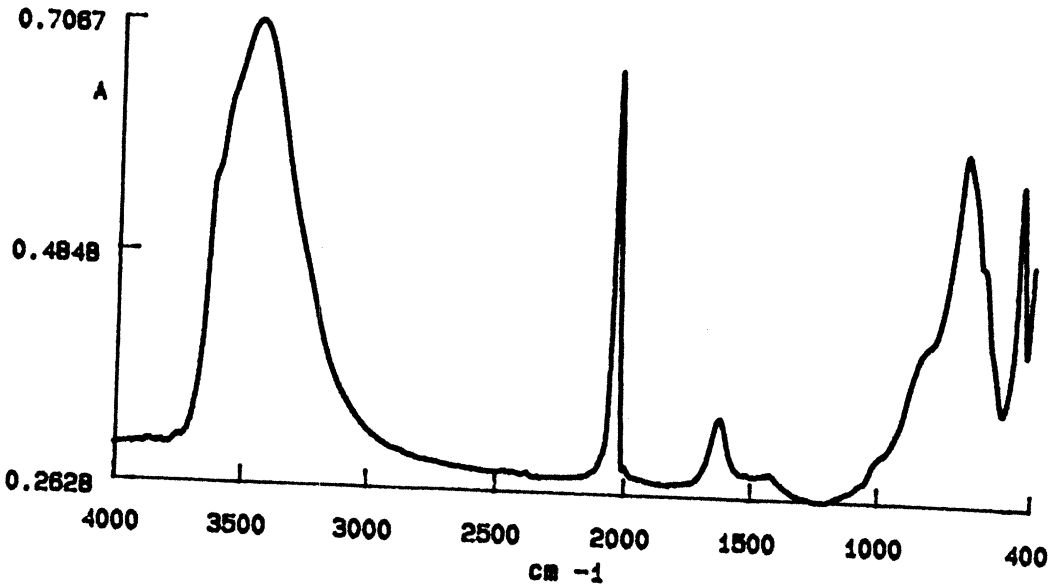

Fig 3.4 FTIR Spectrum of $Mg_2Al(OH)_6[Fe(CN)_6]_{1/4}$, by exchange of $Mg_2Al(OH)_6Cl$ with $(NH_4)_4[Fe(CN)_6]$ for 1 day.

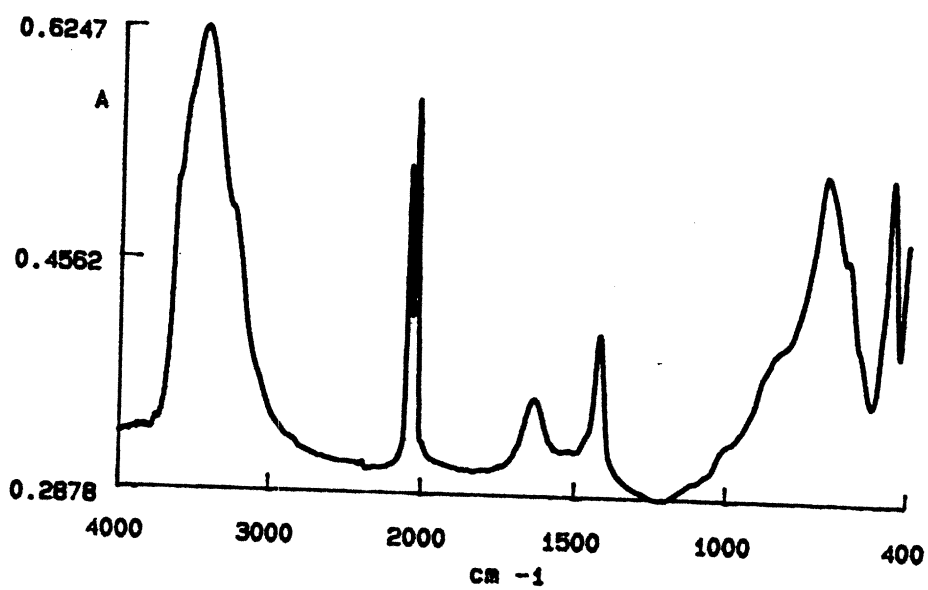

Fig 3.5 FTIR Spectrum of $Mg_2Al(OH)_6[Fe(CN)_6]_{1/4}$ by exchange of $Mg_2Al(OH)_6Cl$ with $(NH_4)_4[Fe(CN)_6]$ for 5 days.

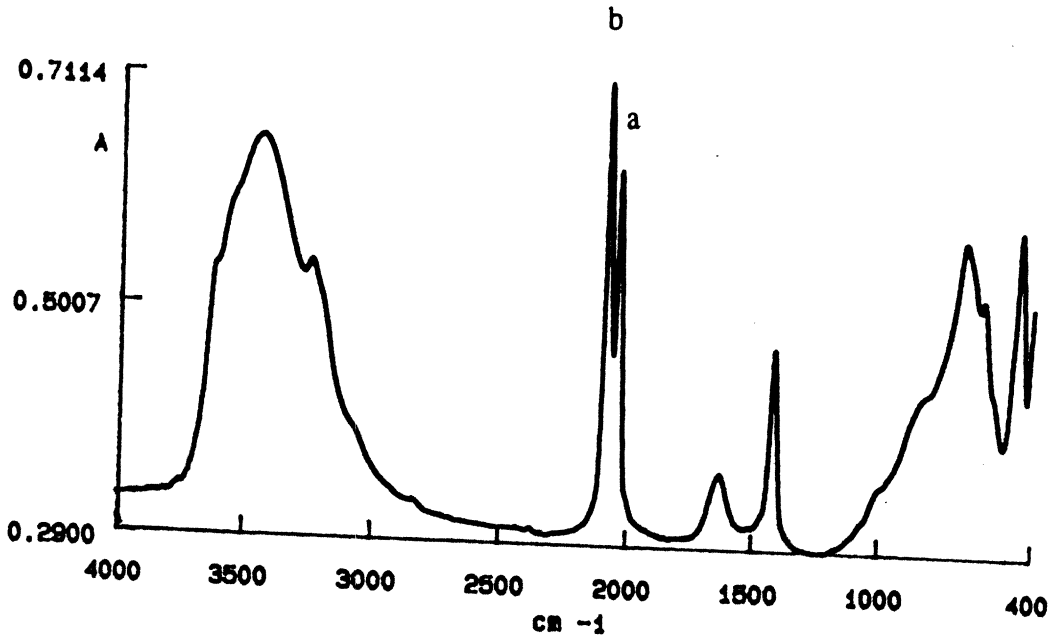

Fig 3.6 FTIR Spectrum of $Mg_2Al(OH)_6[Fe(CN)_6]_{1/4}$ by exchange of $Mg_2Al(OH)_6Cl$ with $(NH_4)_4[Fe(CN)_6]$ for 8 days.

more than one kind of ferrocyanide species in the LDH layers. Further examination of Fig 3.6 led us noticed that two additional peaks appeared, at 3200 and 1416 cm^{-1}, which are assigned to the stretching and bending vibration between N and H in the ammonium ion (1,3,6) (It is discussed further in a later section). This implies that we had not only intercalated new anions (ferrocyanide) by exchange but also included new cations (ammonium).

The co-existence of ammonium and ferrocyanide in the layers makes us draw a connection between these two ions. It is reasoned out that there were two sorts of ferrocyanide: one was those introduced through expected anion exchange, which

substituted the original anions (in this case Cl^-), while the other entered the space between layers, accompanied with ammonium cation, as a neutral molecule. It is suggested that the process happen in two steps: the ferrocyanide first replace the Cl^- in the framework since Cl^- were ready to go; after most of the accessible Cl^- have been substituted the ammonium ferrocyanide in the solution got into the space between the layers. As the ferrocyanides were in different environment, these two species displayed different absorption frequencies in FTIR. The fact that the peaks related to ferrocyanide (peak b) and ammonium ions simultaneously appeared and came to be significant with the time seems to support our suggestions.

In case of the potassium ferrocyanide, there was only one kind of ferrocyanide between the layers. Like most cations, potassium ion is not so easy as ammonium ion to get into the layers (see section 3.3.1.2). The FTIR shows only one peak which displayed no significant difference after 1 and 8 days exchange: the peak b at 2085 cm^{-1} was slightly more intense in the case of 8 days than that of 1 day, and shows little further change.

Figs 3.7-3.8 represent the XRD traces and Tables 3.2-3.3 show the corresponding data of the same samples obtained after 2 days exchange by $(NH_4)_4[Fe(CN)_6]$ and $K_4[Fe(CN)_6]$ respectively. It was noticed that in both cases there were no patterns for $Mg_2Al(OH)_6Cl$ (normally having 2θ = 11.78, 23.48; d_{003} = 0.75nm (16,17)), which implies the complete replacement of Cl^- by ferrocyanide ion. For that exchanged with $(NH_4)_4[Fe(CN)_6]$ (Fig 3.7) there were two sets of spacings: one could be assigned to the pattern in which ferrocyanide replaced Cl^- anion and entered LDH framework

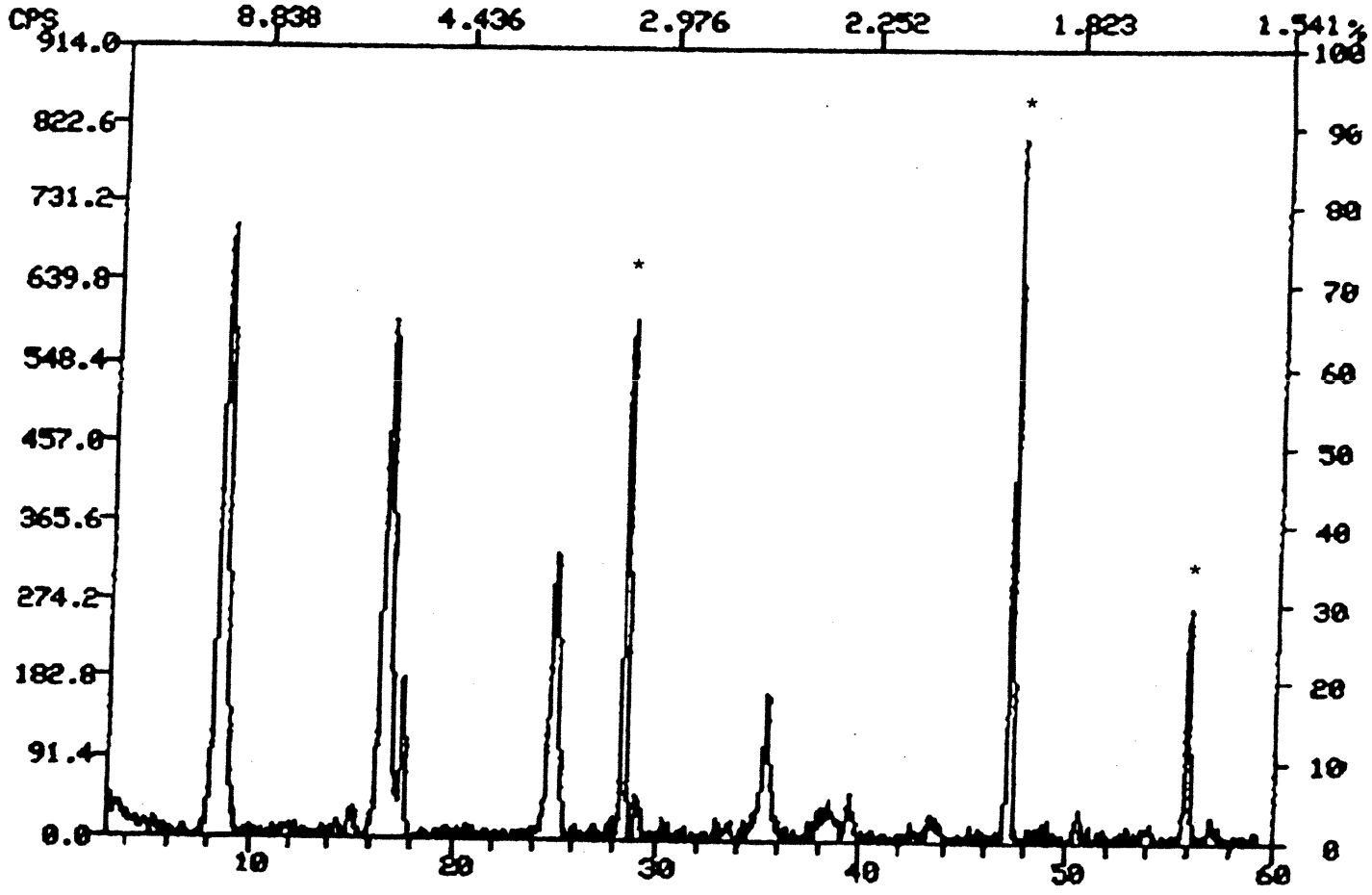

Fig 3.7 XRD trace of $Mg_2Al(OH)_6[Fe(CN)_6]_{1/4}$, obtained by 2 days exchange of $Mg_2Al(OH)_6Cl$ with $(NH_4)_4[Fe(CN)_6]$

(* -- CaF_2 reference)

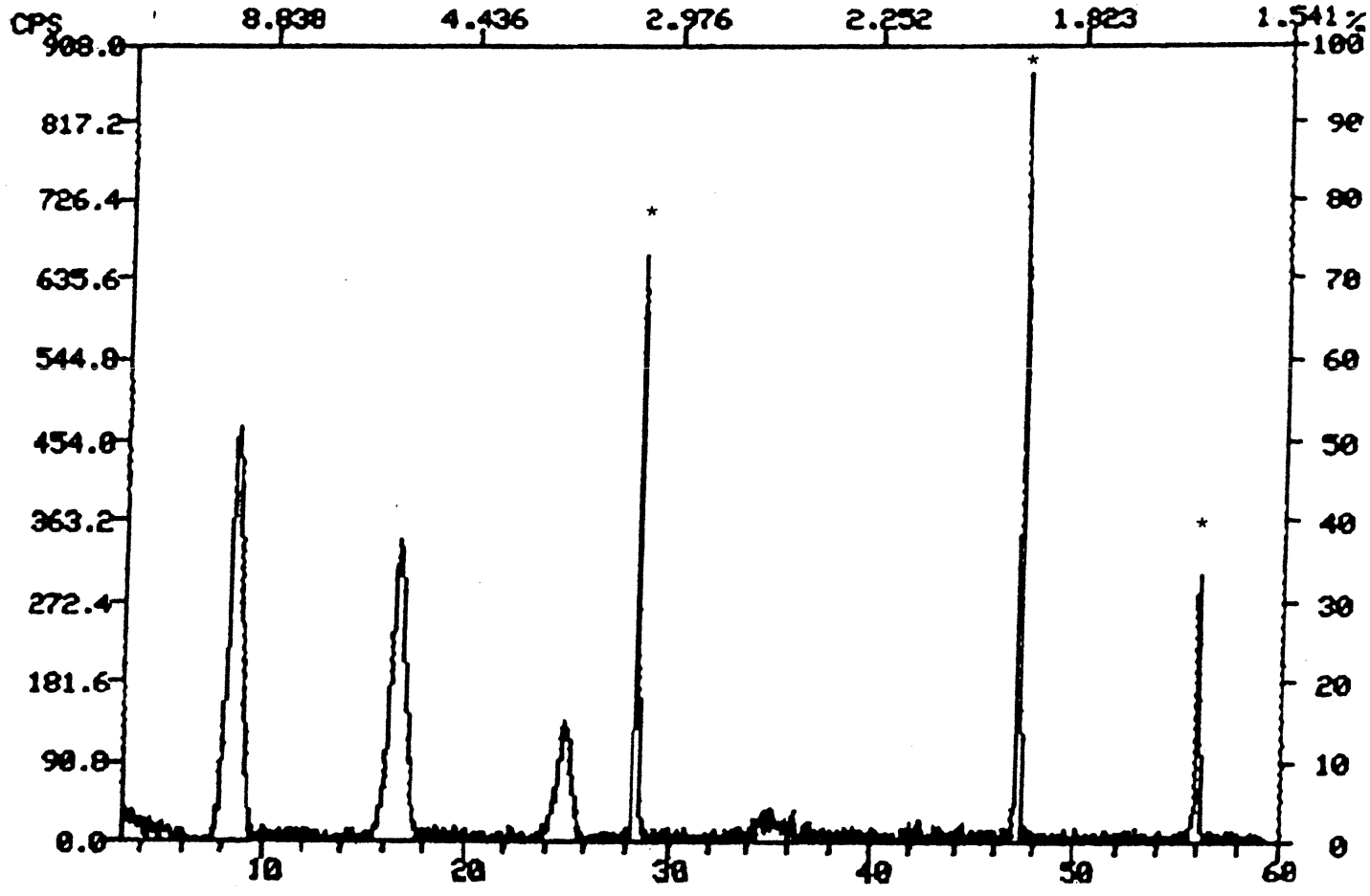

Fig 3.8 XRD trace of $Mg_2Al(OH)_6[Fe(CN)_6]_{1/4}$, obtained by 2 days exchange of $Mg_2Al(OH)_6Cl$ with $K_4[Fe(CN)_6]$

(* -- CaF_2 reference)

Table 3.2 XRD data of $Mg_2Al(OH)_6[Fe(CN)_6]_{1/4}$, obtained by 2 days exchange of $Mg_2Al(OH)_6Cl$ with $(NH_4)_4[Fe(CN)_6]$

2θ	best d (Å)	rel.int.
8.443	10.464	85
16.648	5.321	73
17.539	5.052	22
24.906	3.572	40
35.310	2.540	21

(rel.int.---- relative intensity, same as in the following Tables)

Table 3.3 XRD data of $Mg_2Al(OH)_6[Fe(CN)_6]_{1/4}$, obtained by 2 days exchange of $Mg_2Al(OH)_6Cl$ with $K_4[Fe(CN)_6]$

2θ	best d (Å)	rel.int.
8.560	10.326	100
16.726	5.296	75
24.998	3.559	34

(2θ = 8.88, 16.65, 24.90, d_{003} = 1.05 nm (16)) while the other might relate to that in which ferrocyanide entered as neutral molecule (2θ = 17.54, 35.21). In contrary, for that exchanged with $K_4[Fe(CN)_6]$ (Fig 3.8) there was only one pattern: ferrocyanide entered the layer by replacing Cl^- in the framework (2θ = 8.88, 16.65, 24.90). This result further demonstrated that ammonium ferrocyanide gave two types of materials while potassium ferrocyanide gave only one.

3.3.1.2 Exchange of CO_3^{2-}-formed LDHs with Ferrocyanide salts

3.3.1.2.1 Differences between Potassium and Ammonium ferrocyanide

With its higher charge density, CO_3^{2-} in CO_3-formed LDH is not as easy to be replaced as Cl^-. Figs 3.9-3.10 show the FTIR of the sample after exchange of $Mg_2Al(OH)_6(CO_3)_{1/2}$ with $(NH_4)_4[Fe(CN)_6]$ for 13 days and 50 days, while Fig 3.11 revealed those exchanged with $K_4[Fe(CN)_6]$ for 28 days respectively.

Compared to Cl-formed LDHs, it was more difficult for ferrocyanide to enter the CO_3^{2-}-formed LDHs. This seemed especially true in the case of $K_4[Fe(CN)_6]$: there was little ferrocyanide intercalated even after 28 days exchange. Nevertheless, if $(NH_4)_4[Fe(CN)_6]$ was used, the ferrocyanide ion was able to enter the layers. The noticeable difference from Cl-formed LDH is that the peak at 2025 cm^{-1} appeared quite weak, which still being low even after 50 days exchange. In contrary, the peak around 2085 cm^{-1} came to be more and more significant. In addition, the peak for CO_3^{2-} group at 1360 cm^{-1}(1) remained roughly unchanged. Based upon the assumption in section 3.1.1.1, it is likely, in this case, that the ferrocyanide intercalated were mostly accompanied by ammonium ions, with only limited amount that replaced

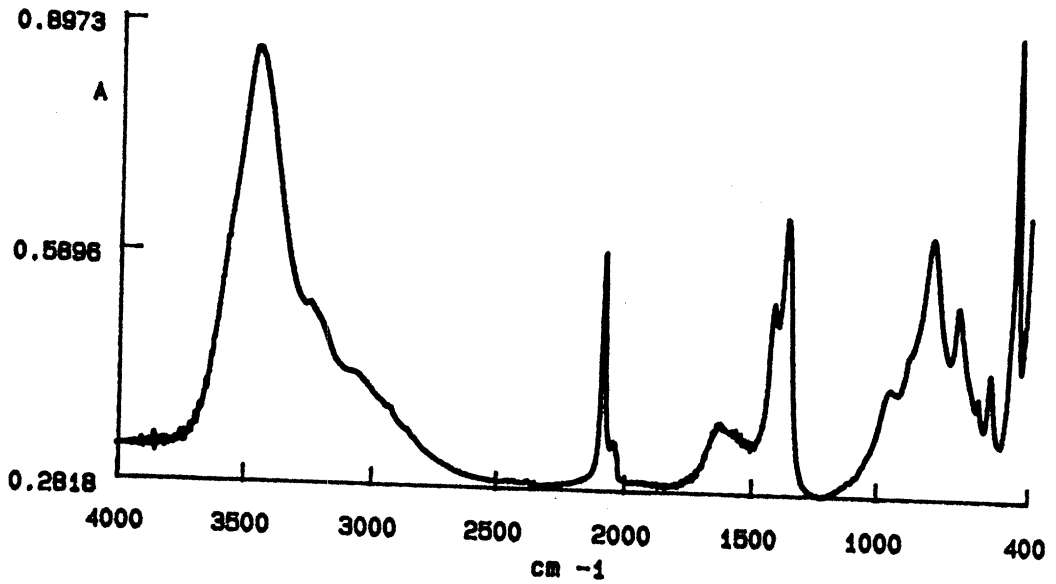

Fig 3.9 FTIR Spectrum of $(NH_4)_4[Fe(CN)_6]$-exchanged $Mg_2Al(OH)_6(CO_3)_{1/2}$, exchanged for 13 days.

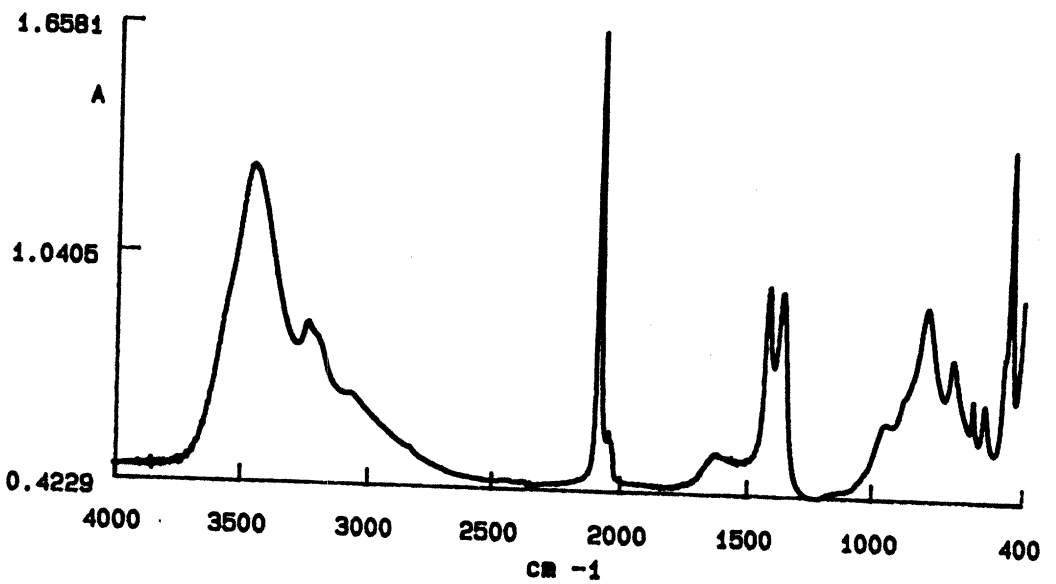

Fig 3.10 FTIR Spectrum of $(NH_4)_4[Fe(CN)_6]$-exchanged $Mg_2Al(OH)_6(CO_3)_{1/2}$, exchanged for 50 days.

carbonate ions and entered between the hydroxylated sheets. This situation indicates that CO_3^{2-} ions, with higher charge density, were strongly bonded on LDH framework.

The reason that $(NH_4)_4[Fe(CN)_6]_{1/4}$ was more readily included than $K_4[Fe(CN)_6]_{1/4}$ into layered double spaces is not yet well understood. It seems that the cation of the ferrocyanide played an important role. As a whole process, it is likely that ferrocyanide anions diffused into the layer first; if replaceable anions in the LDH framework were available, the ferrocyanide ion substituted these anions and became a part of the sheet. In the case that the structural anions were hard to replace the migration of ferrocyanide anions into the layer was controlled by cations: if the charge of the anions could be balanced by cations, which being able to get into the space, the migration continued, otherwise it stopped.

Here arises a question: what causes the difference between potassium and ammonium anions? This might be explained by the hydrogen bonding of the ammonium ions to lattice water and/or ferrocyanide (6), which might aid ammonium ions to enter and to stay in the layered space. This ion-pairing mechanism involved in above process could be employed to transport a cation into what is normally an anion exchange material.

3.3.1.2.2 Heating of $Mg_2Fe(OH)_6(CO_3)_{1/2}$ Sample Exchanged with $(NH_4)_4[Fe(CN)_6]$

The sample used in heating was $Mg_2Fe(OH)_6(CO_3)_{1/2}$ which had been exchanged by $(NH_4)_4[Fe(CN)_6]$ for 50 days. Here, I prefer call it ($Mg_2Fe(OH)_6(CO_3)_{1/2}$, $Mg_2Fe(OH)_6[Fe(CN)_6]_{1/4}$) for the reasons discussed below.

Heating of $(NH_4)_4[Fe(CN)_6]$ exchanged $Mg_2Fe(OH)_6(CO_3)_{1/2}$ led some interesting results. Fig 3.12 displays FTIR spectrum of the sample after heating. Comparing it with Fig 3.10, which was the same sample without heating, we can see some significant differences: first, the peaks related to ammonium ion (3200 and 1416 cm^{-1}) almost disappeared; second, by the ferrocyanide peak at 2085 cm^{-1} shrank while the peak at 2025 cm^{-1} became predominant.

Fig 3.13-3.14 and Table 3.4-3.5 display the XRD traces and data for the same samples respectively. Before heating (Fig 3.13) there were several kinds of patterns between the layers, which were related to carbonate (peaks 2, 5, with 2θ = 11.65, 23.70), ferrocyanide in LDH framework (peaks 1, 3, with 2θ = 8.50, 17.04) as well as, possibly, the material containing ammonium ferrocyanide as neutral molecules (peaks 4, 6, with 2θ = 17.51, 35.18, in general with the related material from $Mg_2Al(OH)_6Cl$, section 3.3.1.1 above). Noticed here was the intensity of neutral ammonium ferrocyanide peaks (4,6), which were much stronger than those of ferrocyanide (1,3) in hydroxylated sheet. After heating (Fig 3.14) only the pattern for the exchanged ferrocyanide has left while the others almost disappeared.

If we take the CaF_2 reference as a standard and compare the intensity of those peaks with that of the reference (CaF_2 was 5% in both cases), the conclusion becomes apparent. The relative intensity ratio of neutral ferrocyanide ($I_{neu\ fer}$, 2θ = 17.51), structural ferrocyanide ($I_{str\ fer}$, 2θ = 8.50) and CaF (I_{CaF2}, 2θ = 28.44) before and after heating are demonstrated in Table 3.6.

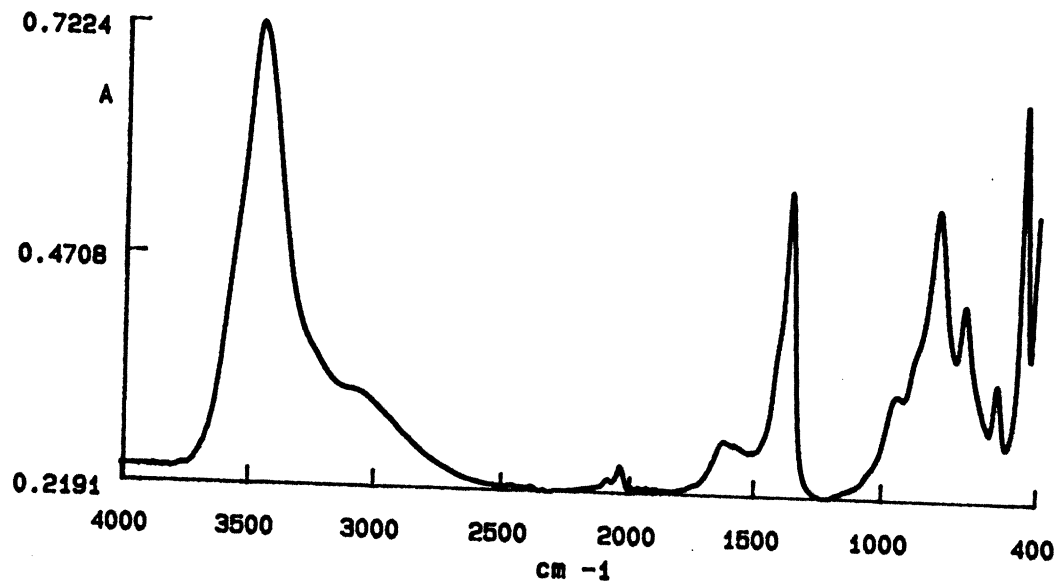

Fig 3.11 FTIR Spectrum of $K_4[Fe(CN)_6]$-exchanged $Mg_2Al(OH)_6(CO_3)_{1/2}$, exchanged for 28 day

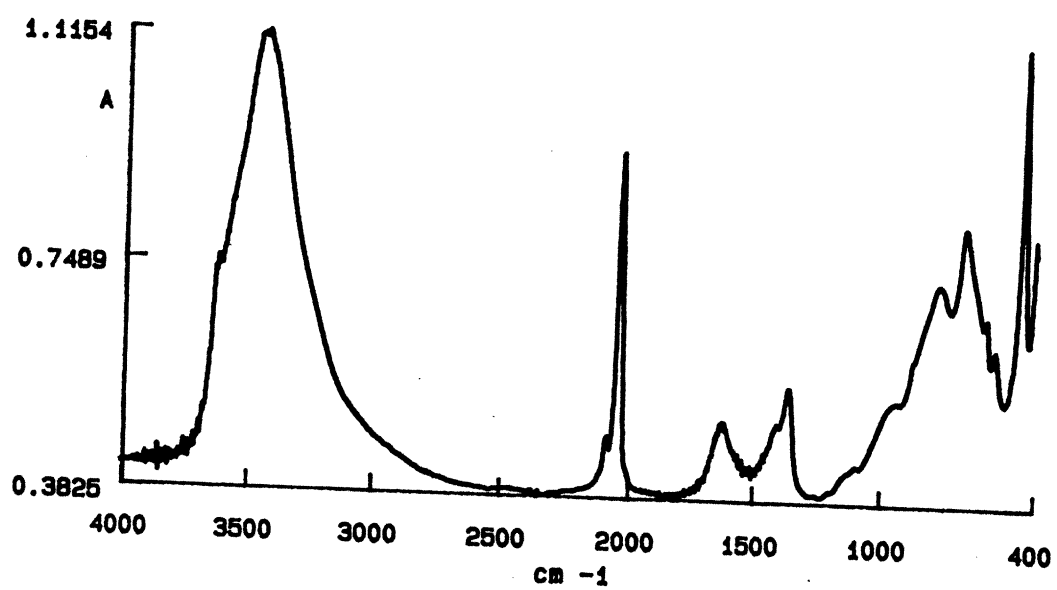

Fig 3.12 FTIR Spectrum of $(NH_4)_4[Fe(CN)_6]$-exchanged $Mg_2Al(OH)_6(CO_3)_{1/2}$, the sample was heated at 95°C for 1 week after 50 days exchange

Before heating (Fig 3.13), the ratio indicated that the ferrocyanide species was largely in forms of neutral molecules. After heating, however, the peaks of the structural ferrocyanide (Fig 3.14) increased and appeared predominant while that of neutral ammonium ferrocyanide became almost invisible. The ratio change in Table 3.6 reflected this change. Although the CaF_2 reference could not be used for an

Table 3.4 XRD data of $(NH_4)_4[Fe(CN)_6]$ exchanged $Mg_2Al(OH)_6(CO_3)_{1/2}$, for 50 days

2θ	best d (Å)	rel.int.
8.503	10.391	8
11.646	7.590	63
15.170	5.836	13
17.044	5.198	6
17.513	5.060	80
23.695	3.752	51
24.775	3.591	40
29.114	3.065	13
35.281	2.542	35
39.532	2.278	14

Table 3.5 XRD data of $(NH_4)_4[Fe(CN)_6]$ exchanged $Mg_2Al(OH)_6(CO_3)_{1/2}$, the sample was heated at 95°C for 1 week after 50 days exchange

2θ	best d (Å)	rel.int
8.451	10.455	100
16.712	5.301	70
25.645	3.550	26

Table 3.6 Relative intensity ratio of XRD patterns, $(NH_4)_4[Fe(CN)_6]$ exchanged $Mg_2Al(OH)_6(CO_3)_{1/2}$ samples with/without heating.

	$I_{neu\ fer}$	$I_{str\ fer}$	I_{CaF}
before heating	1.013	0.147	1.000
after heating	0.120	2.364	1.000

accurate quantitative analysis, the difference between these two relationship is significant enough to indicate a conversion process.

As there was no external source of ferrocyanide ions available (the precipitates had been washed before heating) in the mixture, the only ferrocyanide supplies for the conversion could be those neutral ferrocyanide species between the layers. This result

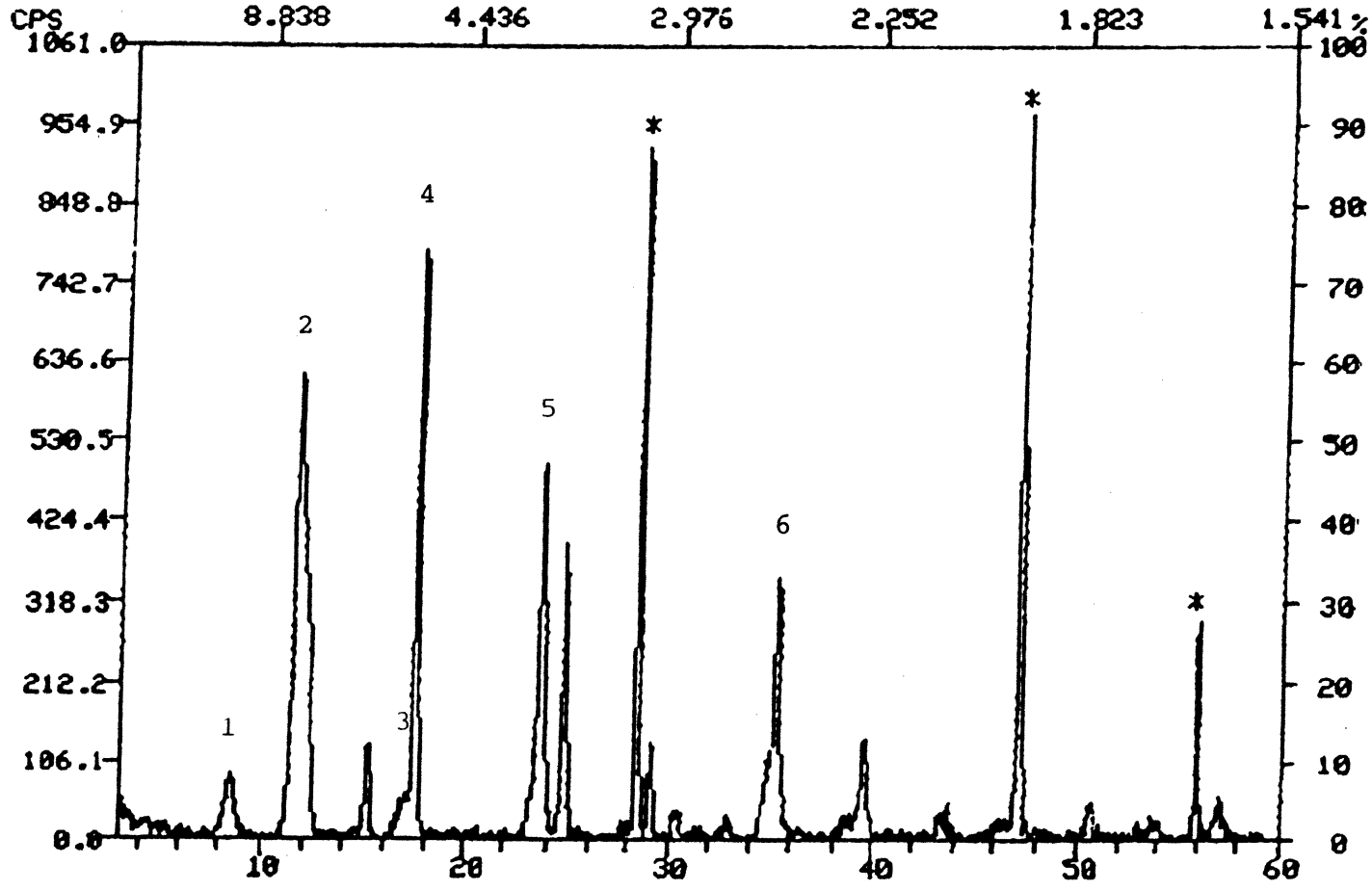

Fig 3.13 XRD trace of $(NH_4)_4[Fe(CN)_6]$ exchanged $Mg_2Al(OH)_6(CO_3)_{1/2}$, exchanged for 50 days. (* - CaF_2 reference)

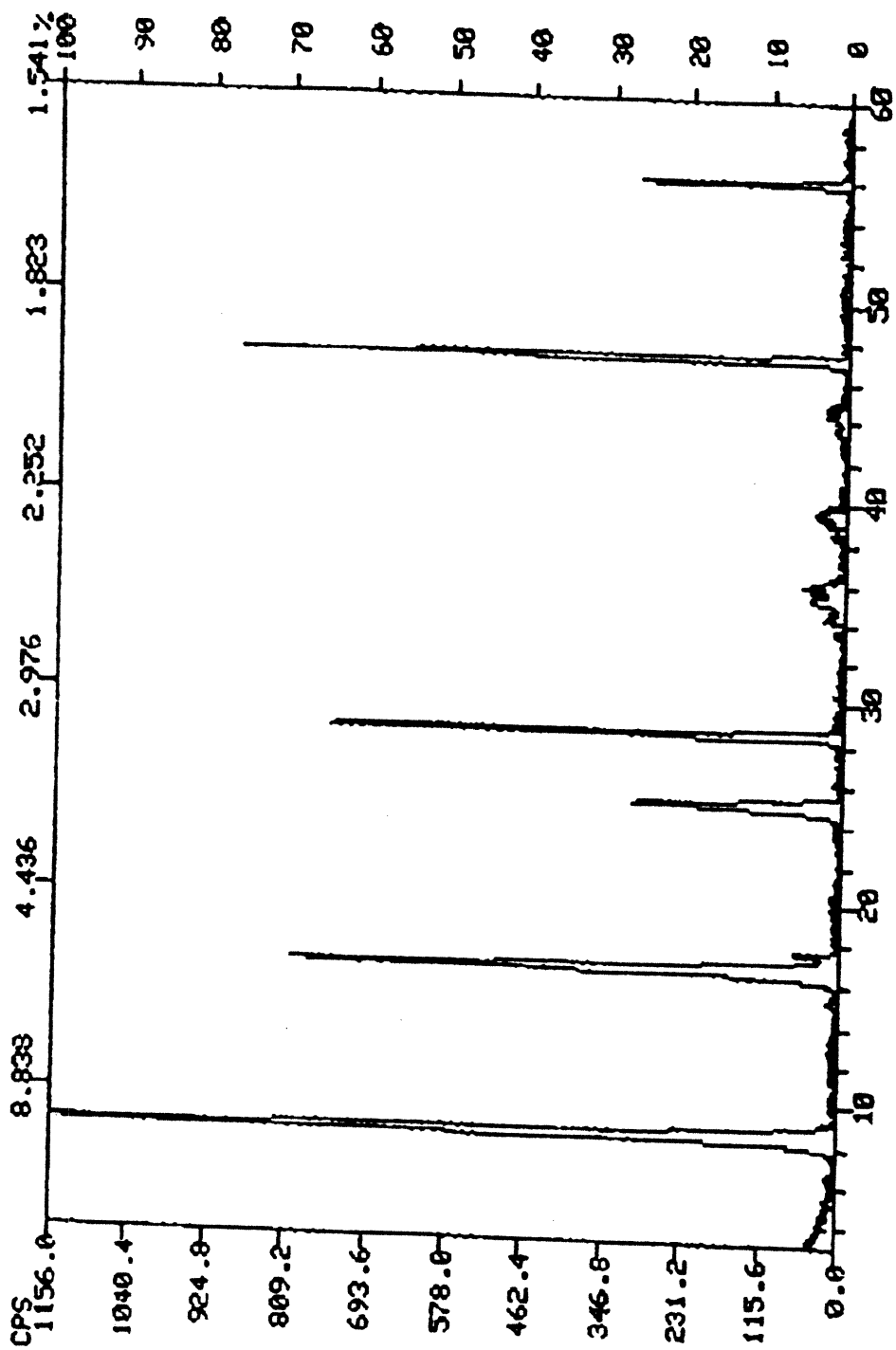

Fig 3.14 XRD trace of $(NH_4)_4[Fe(CN)_6]$-exchanged $Mg_2Al(OH)_6(CO_3)_{1/2}$; the sample was heated at 95°C for 1 week after 50 days exchange. (* - CaF_2 reference)

strongly suggested the existence of non-structural ferrocyanide and the conversion of non-structural to structural ferrocyanide.

So far, both FTIR and XRD indicated the possibility of removal of carbonate from LDHs by ferrocyanide. A passible process could be as follows. Before heating, the LDH was almost still in carbonate form (that is why at the beginning of this section I still call the sample $Mg_2Fe(OH)_6(CO_3)_{1/2}$); only small amount of ferrocyanide replaced the carbonate and entered LDH framework while most intercalated ferrocyanide species were neutral molecules. After heating gently for 1 week, the LDH lost most carbonate and ammonium for the outgoing diffusion from LDH and, then, evaporation of CO_2 and NH_3. The vacancies left in LDHs, because of removal of carbonate, were filled by ferrocyanide ions. In other words, driven by thermodynamic enthalpy, the carbonate ions, which had lower charge density, were replaced by ferrocyanide. The FTIR changes on Fig 3.12 from Fig 3.10 might also reflect this processes.

The significance of above process is not only the replacement of ferrocyanide to carbonate but, more significantly, the remaining of CO_3^{2-} in the ferrocyanide exchanged LDH spacing. Fig 3.12 reveals the presence of CO_3^{2-} ions (1360 cm^{-1}), which does not show in XRD trace (Fig 3.14). An explanation is that the CO_3^{2-} ions lie between the layer occupied by ferrocyanide ion. Therefore, the XRD only displays the spacing determined by ferrocyanide, not by the CO_3^{2-}. Besides, this process also provides the possibility of deriving a new LDH, with expected anions, from CO_3^{2-}-

formed LDHs provided the ammonium salt of that anion is available. These results might be somewhat meaningful in the studies of origin of life.

3.3.2 Sulfate-formed LDHs (SO_4^{2-}-LDHs)

SO_4^{2-}-LDHs have the formula as $[M^{2+}_2M^{3+}(OH)_6](SO_4)_{1/2}$ (where $M^{2+} = Mg^{2+}$; $M^{3+} = Al^{3+}$, Fe^{3+}). I used two ways to obtain these SO_4^{2-}-LDHs. One way was intercalation of SO_4^{2-} through direct synthesis or anion exchange, while the other was by introducing S^{2-} (either by anion exchange or direct synthesis) into a LDH and then oxidizing S^{2-} to transform it to a sulfate-formed LDH by using H_2O_2. In the latter case Cl^--formed LDHs would be a suitable choice for anion exchange.

Figs 3.15-3.16 exhibit the FTIR spectra for $[Mg_2Fe(OH)_6](SO_4)_{1/2}$ and $[Mg_2Al(OH)_6](SO_4)_{1/2}$. The former was obtained by exchanging SO_4^{2-} anions directly, and the latter by oxidation schemes. The peak around 1116 cm^{-1} on both figures indicates the existence of the SO_4^{2-} group(1,17). However, if the S^{2-} method was employed to obtain $[Mg_2Fe(OH)_6](SO_4)_{1/2}$ the process became complicated.

Fig 3.17 is a XRD trace for $[Mg_2Fe(OH)_6](SO_4)_{1/2}$ by direct exchange of SO_4^{2-} with $[Mg_2Fe(OH)_6]Cl$, with corresponding XRD data in Table 3.7. The XRD patterns reveals crystal structure in the material. Fig 3.18 represents the XRD of that obtained through S^{2-} exchange and oxidation. Comparing these two figures we can see that the peaks in Fig 3.18 became rather weak, almost buried in instrument noise, which indicates poor crystallinity. A possible reason is that, in the process of S^{2-} intercalation, the sulfide anions attacked the Fe^{3+} in the LDH and formed Fe_2S_3 precipitate, which isolated the Fe^{3+} from the layers and destroyed the crystal structures.

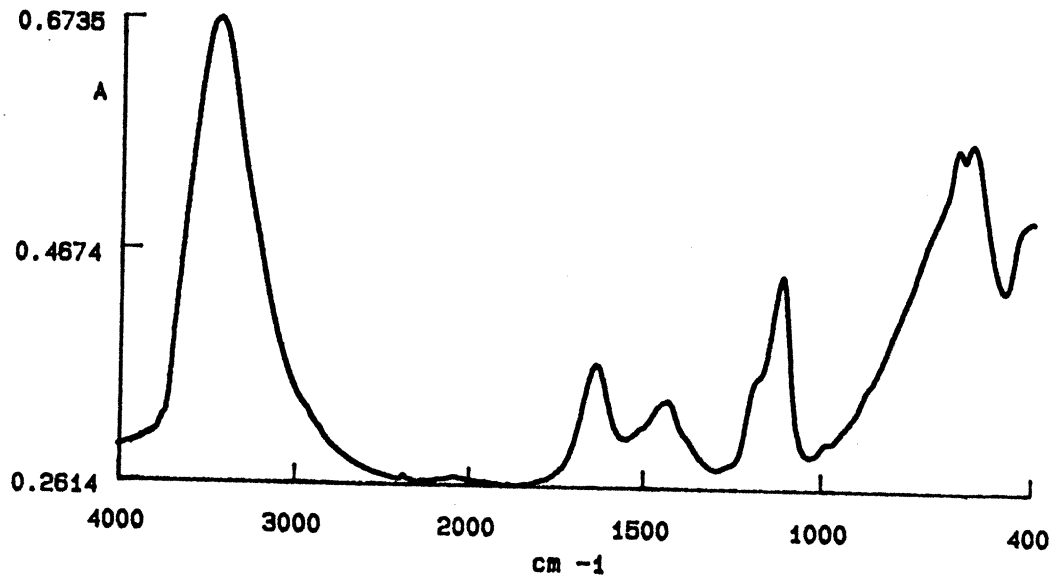

Fig 3.15 FTIR spectrum of $[Mg_2Fe(OH)_6](SO_4)_{1/2}$, obtained by exchange of SO_4^{2-} with $Mg_2Fe(OH)_6Cl$

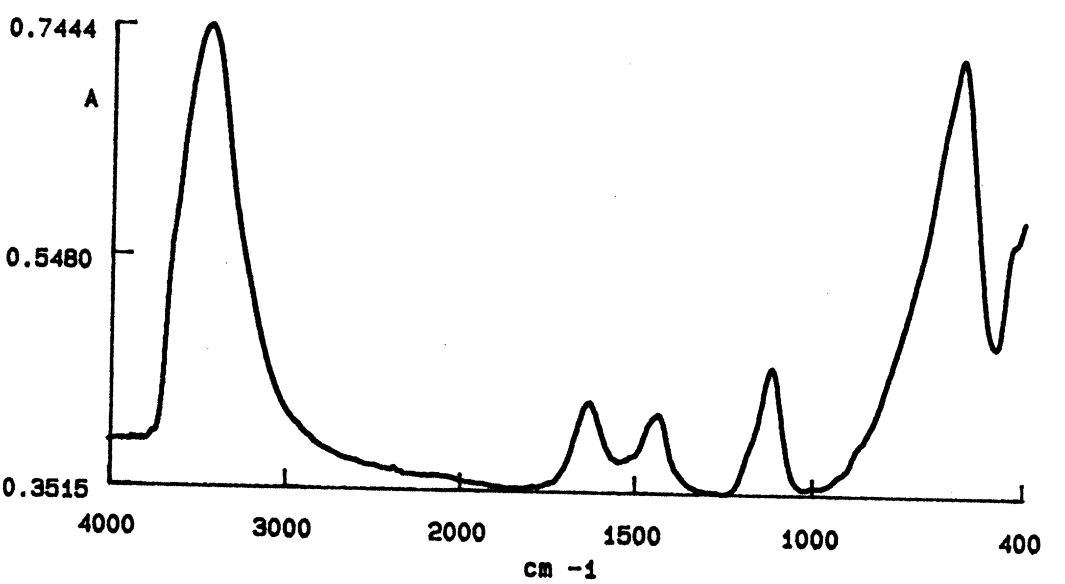

Fig 3.16 FTIR spectrum of $[Mg_2Al(OH)_6](SO_4)_{1/2}$, obtained through oxidation of $[Mg_2Al(OH)_6]S_{1/2}$

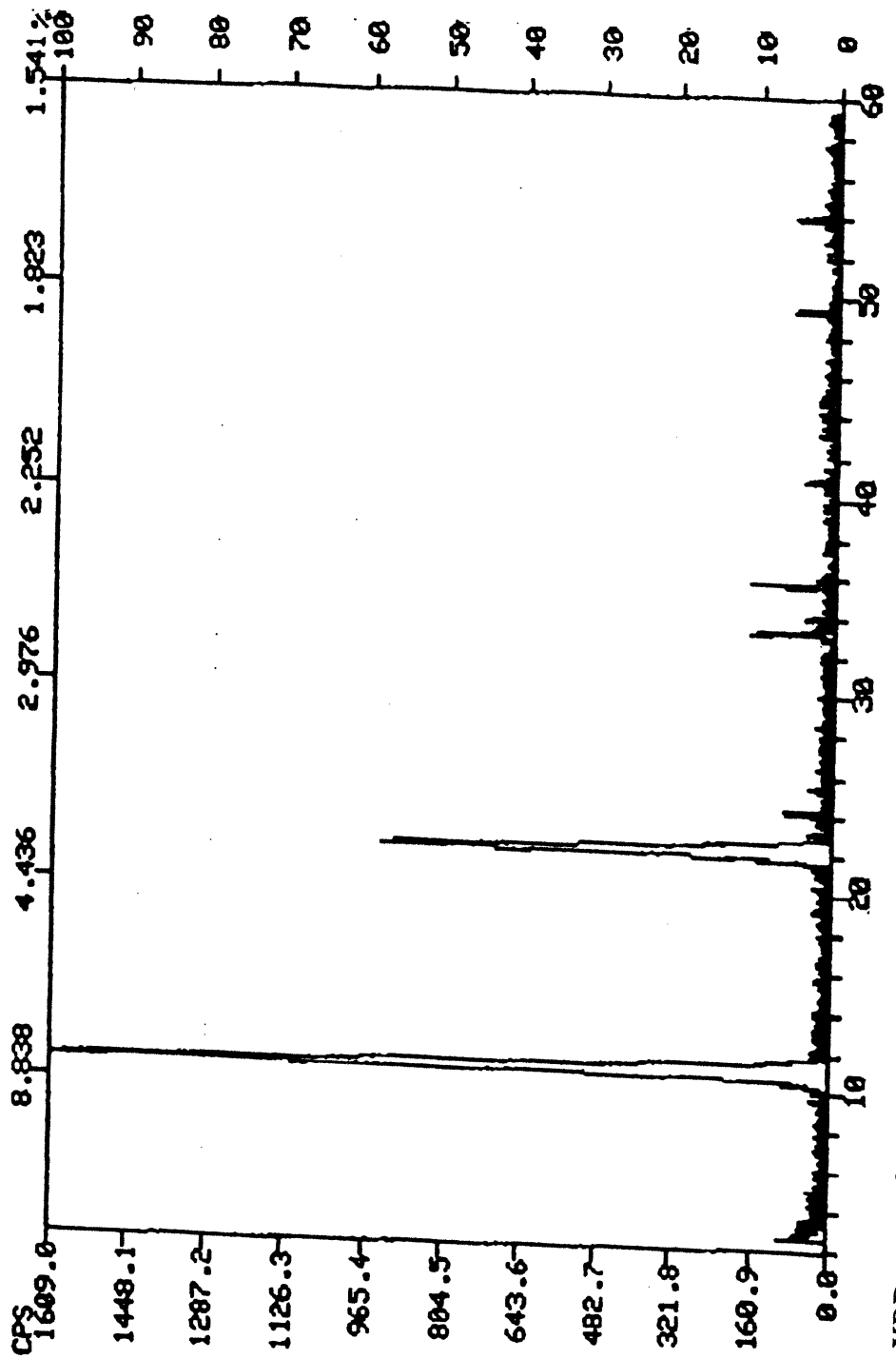

Fig 3.17 XRD trace of $[Mg_2Fe(OH)_6](SO_4)_{1/2}$, obtained through exchange of SO_4^{2-} with $Mg_2Fe(OH)_6Cl$.

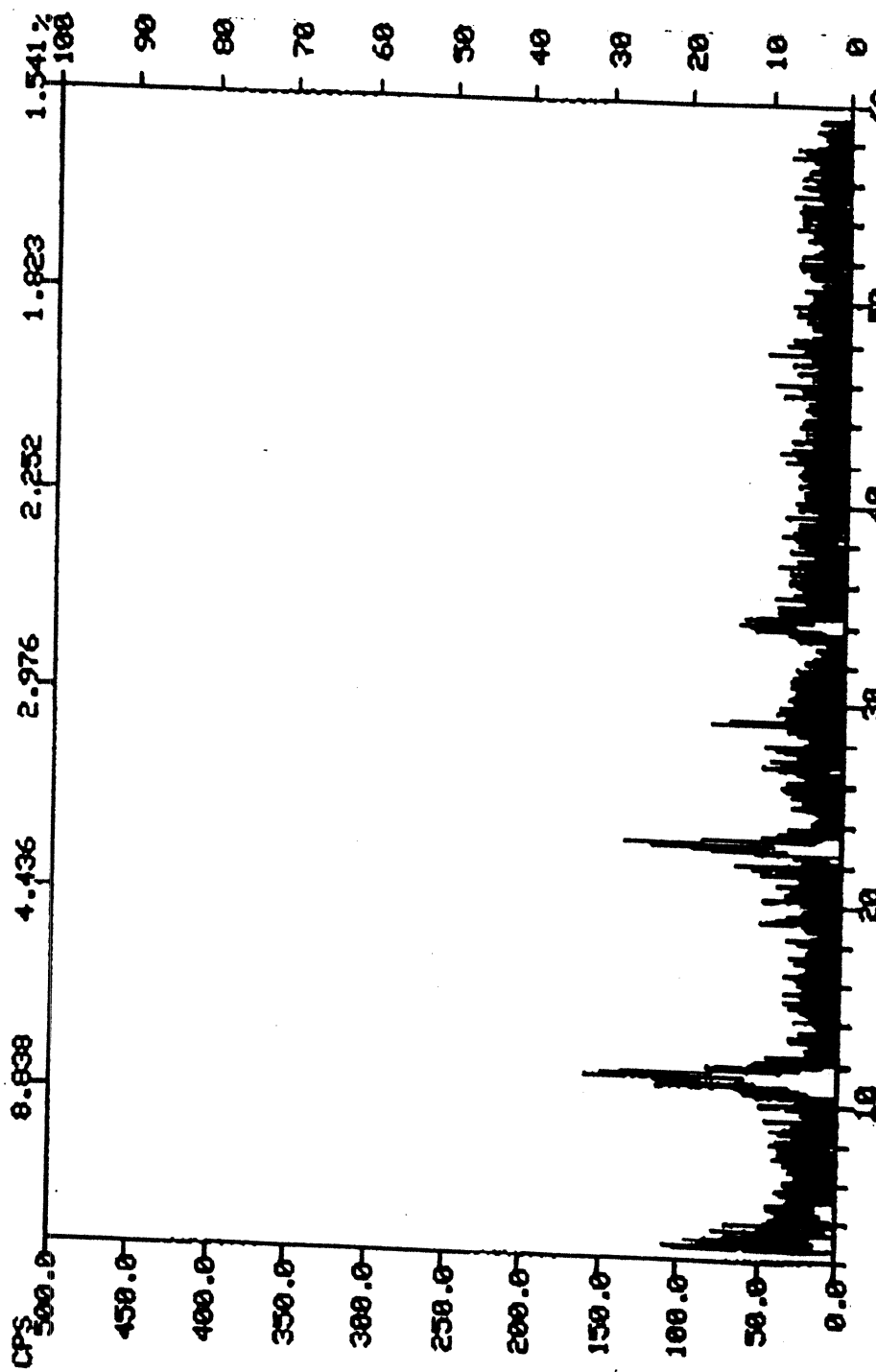

Fig 3.18 XRD trace of $[Mg_2Fe(OH)_6](SO_4)_{1/2}$, obtained through S^{2-} exchange with $Mg_2Fe(OH)_6Cl$ (without annealing) followed by oxidation

The observation that after adding Na_2S solution to $[Mg_2Fe(OH)_6]Cl$ suspension the light brownish LDH suspension gradually became blackish might indicate the formation of Fe_2S_3.

However, if we annealed the $[Mg_2Fe(OH)_6]Cl$ at 140°C for 1 week before exchanging it with S^{2-}, things became somewhat different. Fig 3.20 and Table 3.8 show the XRD trace and data of the sample prepared from $Mg_2Al(OH)_6Cl$ annealed on

Table 3.7 XRD data of $[Mg_2Fe(OH)_6](SO_4)_{1/2}$, by direct exchange of SO_4^{2-} with $[Mg_2Fe(OH)_6]Cl$

2θ	best d (Å)	rel.int
11.635	7.600	100
23.138	3.841	49

Table 3.8 XRD data of $Mg_2Fe(OH)6S_{1/2}$, by exchange of $Mg_2Fe(OH)_6Cl$ (annealed) with S^{2-}.

2θ	best d (Å)	rel.int
11.075	7.982	100
22.186	4.003	57

140°C for 7 days before exchange, while Fig 3.19 shows that obtained without annealing. Obviously the former one substantially retained more crystal structure than the later one. This result indicated a possibility to protect LDH structure, by annealing, from the attack of S^{2-}. It is likely that after annealing at high temperature the LDH became more structurally oriented and contained larger crystal particles; this process could effectively decrease the amount of vulnerable Fe^{3+} ions, which were the targets of S^{2-} attack, by reducing the outer surface area.The color of S^{2-}-exchanged iron-LDH, which had been annealed before exchange, still being brownish might indicate that the crystal structure of $[Mg_2Fe(OH)_6]S_{1/2}$ was largely retained. Fig 3.21 shows the XRD trace of the sample obtained by oxidation of $[Mg_2Fe(OH)_6]S_{1/2}$ annealed before anion exchange. Apparently, the material lost its crystal structure after oxidation. The peaks above 30° (2θ) in Fig 3.21 might related to the intermediates of oxidized products. It is not known what caused the further collapse in the oxidation process. These phenomena revealed that preparation of $[Mg_2Fe(OH)_6](SO_4)_{1/2}$ through H_2O_2 oxidation of S^{2-}-formed iron contained LDH might not be a good method.

3.3.3 Intercalation of Organic Species

Most of our work so far for LDHs has been focused on the area related to inorganic species. Compared to inorganic anions, the intercalation of organic species has been less well studied.

However, with potential applications there is increasing interest in this area (11-14). Since the question whether an organic species can stay in LDH's space is quite important to the study of origin of life, which suggests the conversion at an early

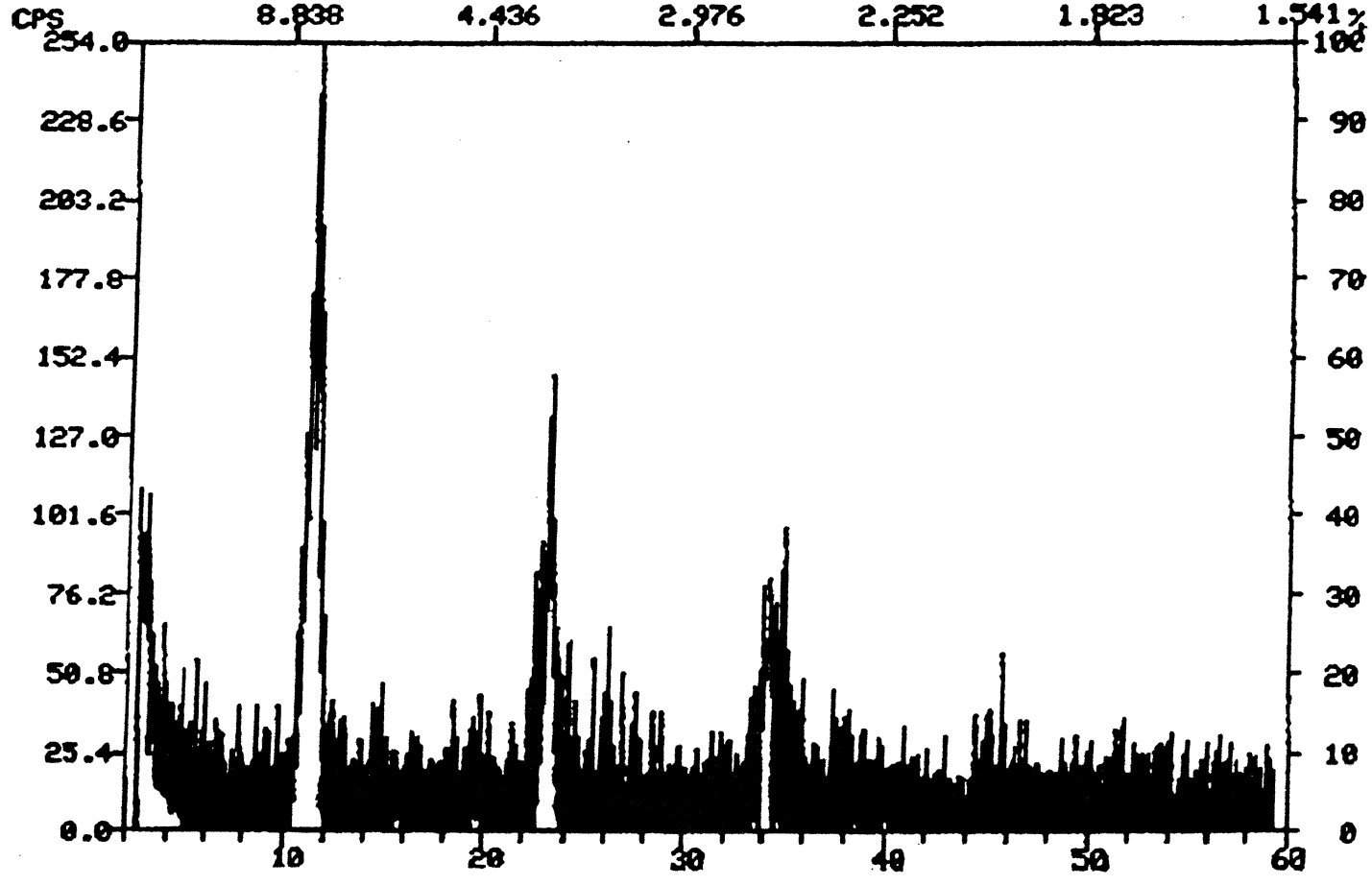

Fig 3.19 XRD trace of $[Mg_2Fe(OH)_6]S_{1/2}$ obtained through anion exchange of Na_2S with $[Mg_2Fe(OH)_6]Cl$, no annealing before exchange

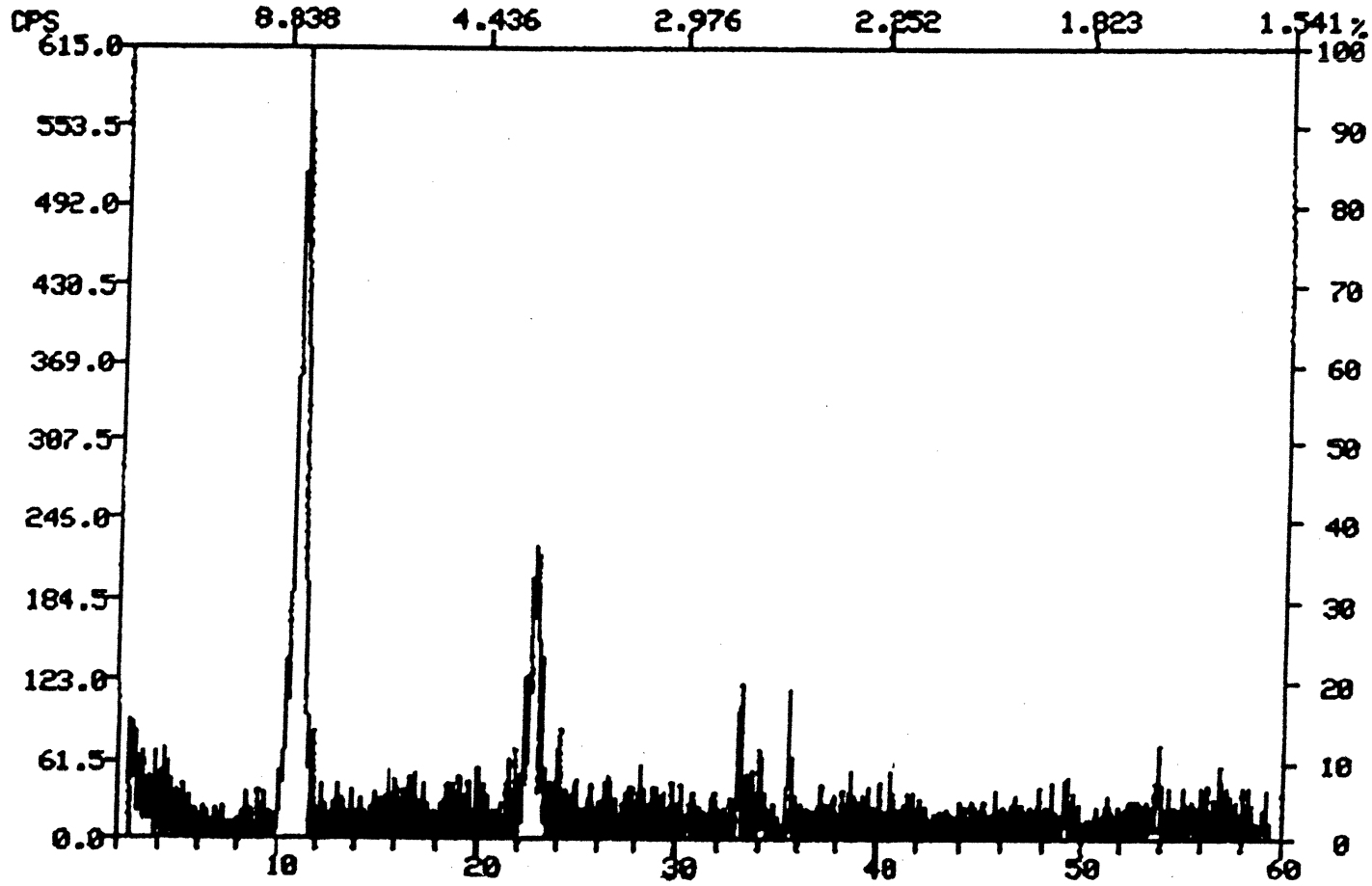

Fig 3.20 XRD trace of $[Mg_2Fe(OH)_6]S_{1/2}$ obtained through anion exchange of Na_2S with $[Mg_2Fe(OH)_6]Cl$, annealed before exchange

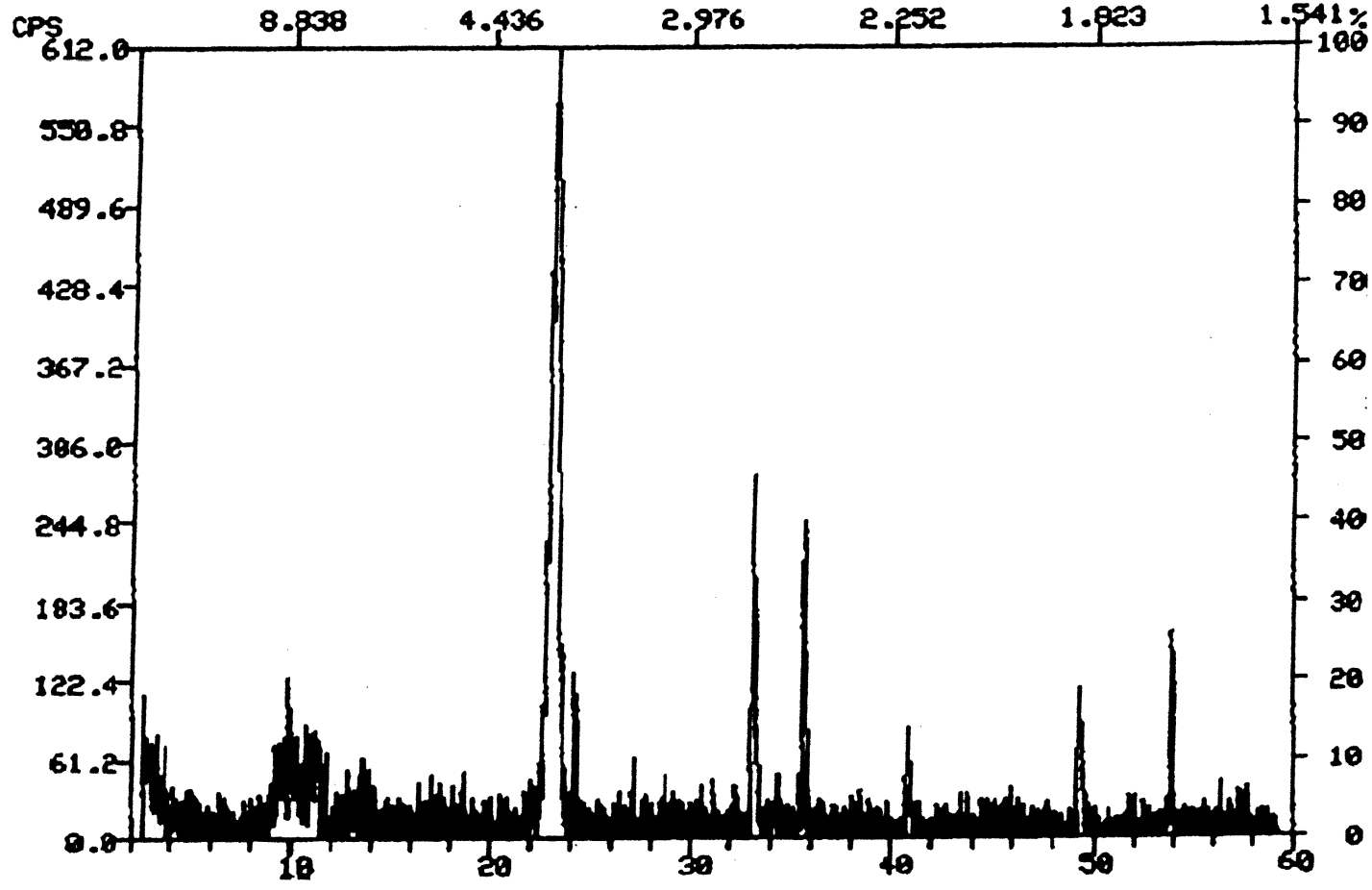

Fig 3.21 XRD trace of $[Mg_2Fe(OH)_6](SO)_{1/2}$ obtained through oxidation of $[Mg_2Fe(OH)_6]S_{1/2}$, sample annealed before anion exchange

evolutionary stage from inorganic species to organic species within LDH's layer, several experiments were arranged to see if some organic species can be intercalated.

3.3.3.1 Synthesis of $[Mg_2M^{3+}(OH)_6](HCOO)$

I used direct synthesis to make $[Mg_2M^{3+}(OH)_6](HCOO)$ (where $M^{3+} = Al^{3+}$ or Fe^{3+}). The reactions were carried out under nitrogen and obtained solid were dried in a nitrogen flushed desiccator. Fig 3.22-3.23 depict the FTIR spectra respectively for $Mg_2Al(OH)_6(HCOO)$ and $Mg_2Fe(OH)_6(HCOO)$. The peak at 1618 cm^{-1} indicated the possible presence of the $HCOO^-$ group (1). With careful examination of the figures we could see a small peak-like curve in the region between 2700-2820 cm^{-1}. By processing the first derivative upon the curve, two peaks, which were believed being related to the stretch vibration of C-H bond (1), were identified at.

Figs 3.24-3.25 and Table 3.9-3.10 display the XRD traces as well as data of $Mg_2Al(OH)_6(HCOO)$ and $Mg_2Fe(OH)_6(HCOO)$ respectively. Both of the precipitates show layered structure. However, the patterns are quite close to that of $Mg_2Al(OH)_6Cl$ and $Mg_2Al(OH)_6(CO_3)_{1/2}$: the best d_{003} is 7.75 for $Mg_2Al(OH)_6(HCOO)$ sample, 7.85 for $Mg_2Fe(OH)_6(HCOO)$, 7.60 for $Mg_2Al(OH)_6Cl$ and 7.59 for $Mg_2Al(OH)_6(CO_3)_{1/2}$. The differences between these are not significant enough to conclusively distinguish one from another. Thus, at this stage, by XRD trace only we could not exclude the possibilities that the synthesized layered structure was $Mg_2Al(OH)_6Cl$.

To solve this question I exchanged the sample of $Mg_2Al(OH)_6(HCOO)$ and $Mg_2Fe(OH)_6(HCOO)$ with NaCl. FTIR of the products show a decrease in the peaks at 1618 cm^{-1}. This confirmed the assignment of this peak being $HCOO^-$ and implied that

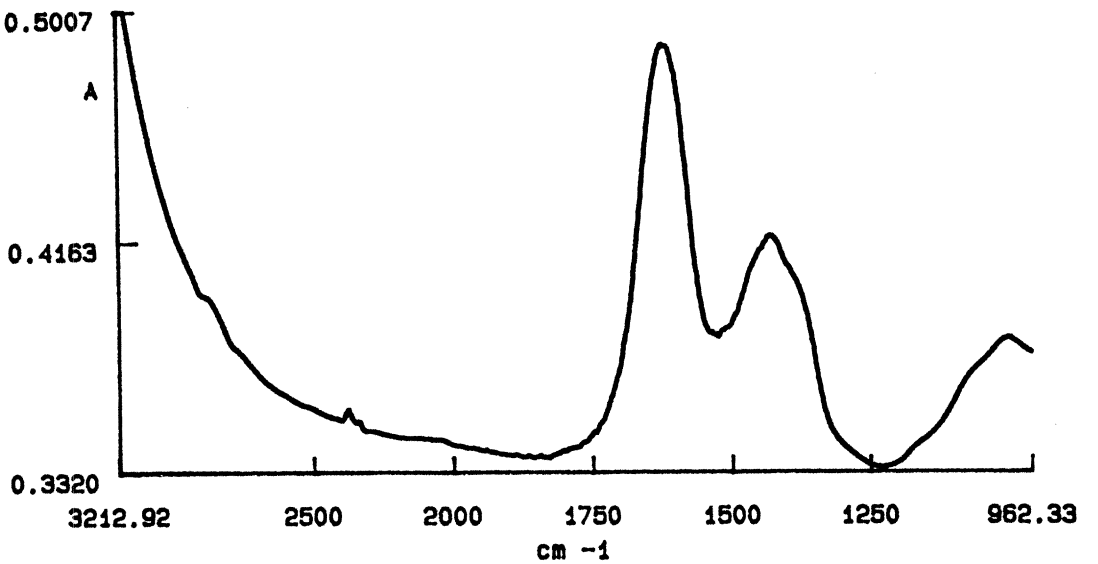

Fig 3.22 FTIR spectrum of $Mg_2Fe(OH)_6(HCOO)$, by direct synthesis

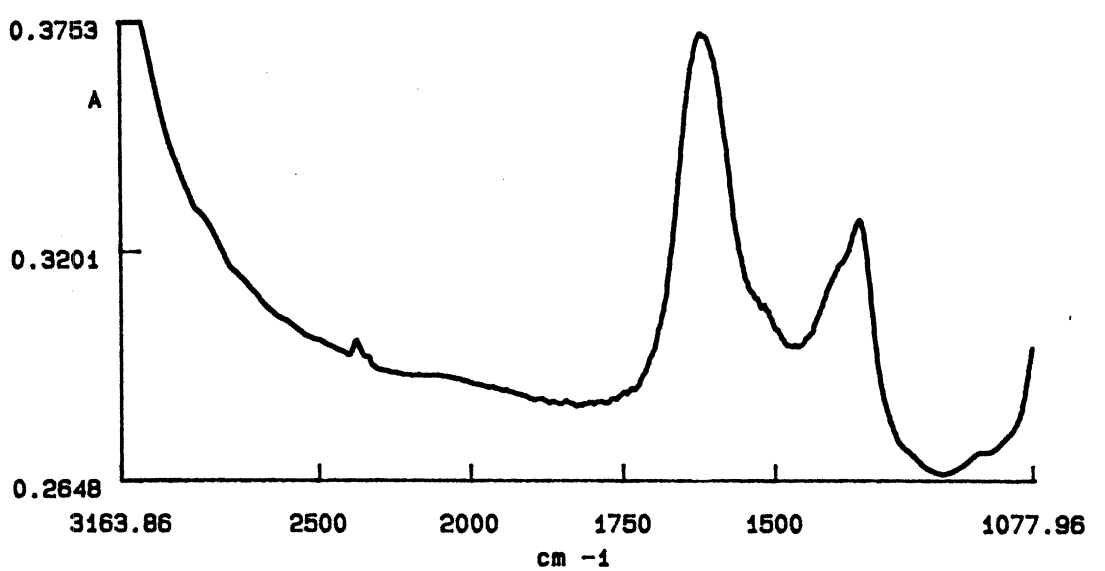

Fig 3.23 FTIR spectrum of $Mg_2Al(OH)_6(HCOO)$, by direct synthesis

Table 3.9 XRD data of $Mg_2Al(OH)_6(HCOO)$, by direct synthesis

2θ	best d (Å)	rel.int.
11.674	7.574	100
23.337	3.809	53
35.248	2.544	4

Table 3.10 XRD data of $Mg_2Fe(OH)_6(HCOO)$, by direct synthesis

2θ	best d (Å)	rel.int
11.309	7.818	100
22.565	3.937	50
34.338	2.609	12

the $HCOO^-$ in $Mg_2Al(OH)_6(HCOO)$ was replaced by Cl^-. The significance of this work is that it provides a possibility to expend our work into organic areas.

3.3.3.2 Attempted Intercalation of HCOH into LDH

Another piece of work I did in this area was try to include HCOH into LDHs by synthesizing $Mg_2Al(OH)_6Cl$ in the presence of HCOH. The purpose was to see if a simple neutral organic molecule could be inserted into the layers. The procedure was

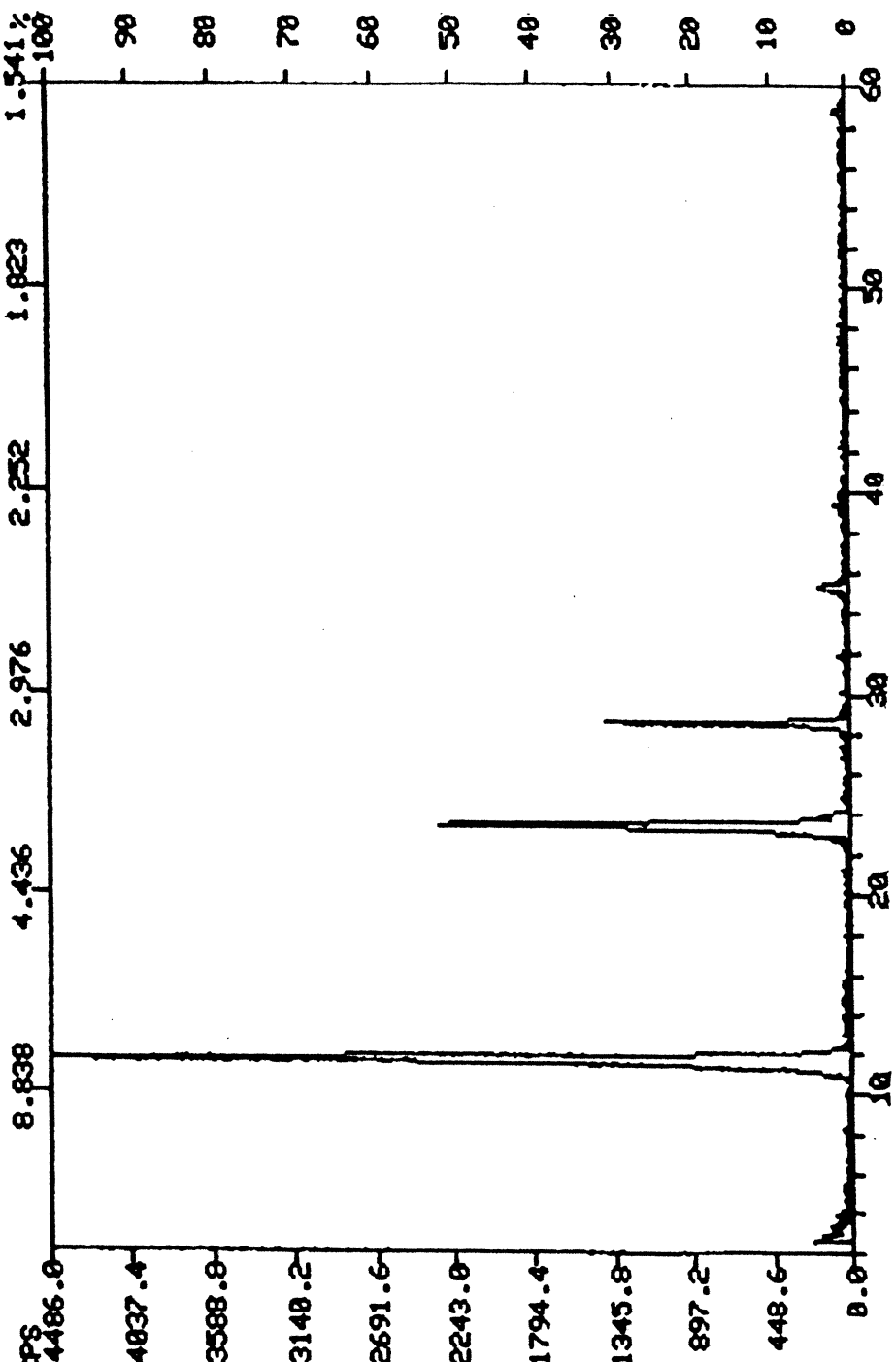

Fig 3.24 XRD trace of $Mg_2Al(OH)_6(HCOO)$, by direct synthesis

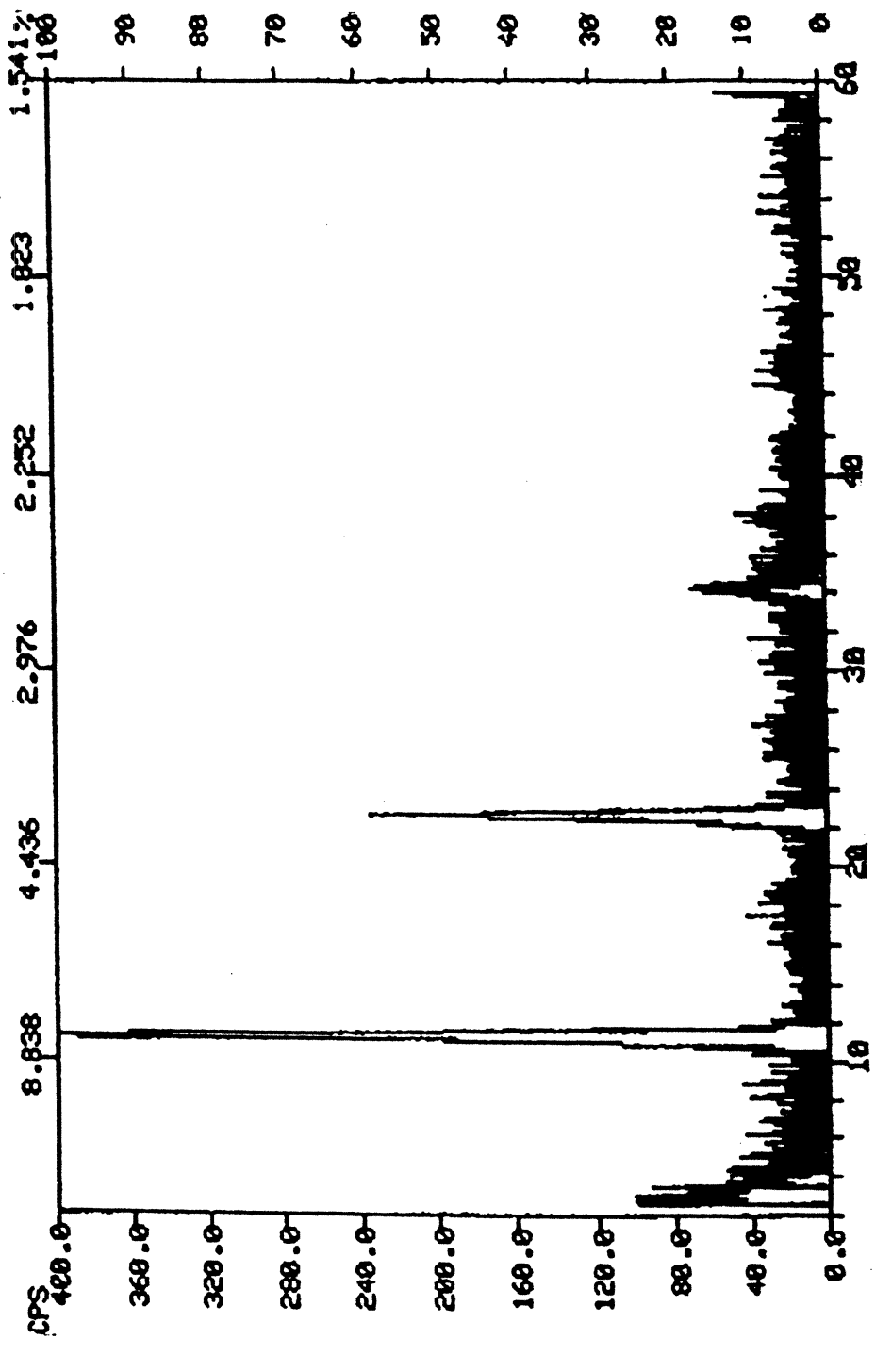

Fig 3.25 XRD trace of $Mg_2Fe(OH)_6(HCOO)$, by direct synthesis

carried out in the usual way except without reflux of the precipitates overnight. A stoichiometric amount of Cl^- was added into the solution, while HCOH/Cl^- ratio was 1.5. The sample obtained was washed, dried and its FTIR spectrum collected is presented in Fig 3.26.

The new peak at 3117 cm^{-1} might be taken as the evidence of intercalation of HCOH. However, it is somewhat higher than expected (2830 and 2750 cm^{-1} for free formaldehyde) (1). The peak at 1620 cm^{-1} might be related to C-O stretching vibration. The XRD patterns in Fig 3.27 and data in Table 3.11 show more than one kind of spacing: one of them could be assigned to $Mg_2Al(OH)_6Cl$ (2θ = 11.77, 23.48), while the other might be different material (2θ = 14.51, 28.01, 38.69, 49.8). These results suggested the intercalation of HCOH. However, the form of HCOH in the layered space is not known. Further work is needed to elucidate it.

3.3.3.3 Synthesis of LDH in the Presence of Ethanolamine

Ethanolamine could also be intercalated into LDHs. The synthesis, in which Mg^{2+} and Al^{3+} were used, was carried out in the same way as the preparation of Cl^--formed LDH except for the omission of excess Cl^- and the inclusion of ethanolamine ($NH_2CH_2CH_2OH$: Al = 4 : 1). The suspension was refluxed for overnight under the protection of nitrogen. The pH was 11.8 and 9.5 before and after the reflux.

The XRD trace and data of the sample are displayed in Fig 3.28 and Table 3.12 respectively. It is noticed that the XRD patterns are quite simple. Apparently, the pattern is not due to $Mg_2Al(OH)_6Cl$ as it largely deviates from those of Cl^--formed LDH. Thus, surely, I had obtained a new material which, possibly, contained

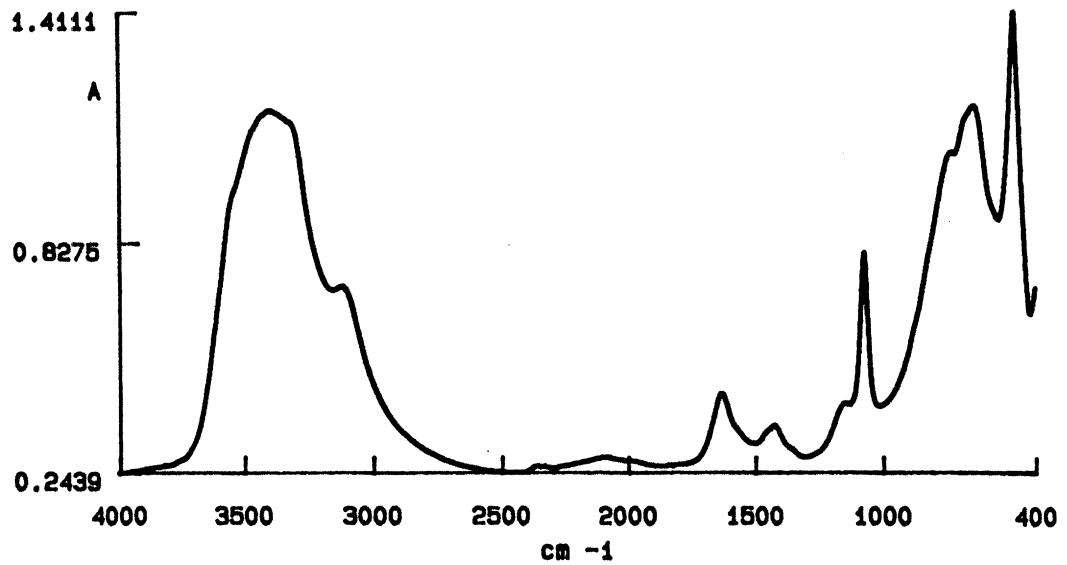

Fig 3.26 FTIR spectrum of $Mg_2Al(OH)_6Cl$, directly synthesized in the presence of HCOH

Table 3.11 XRD data of $Mg_2Al(OH)_6Cl$, directly synthesized in the presence of HCOH

2θ	best d (Å)	rel.int
11.779	7.507	63
14.550	6.085	78
23.479	3.787	30
28.010	3.183	24
38.500	2.330	47
49.110	1.852	45

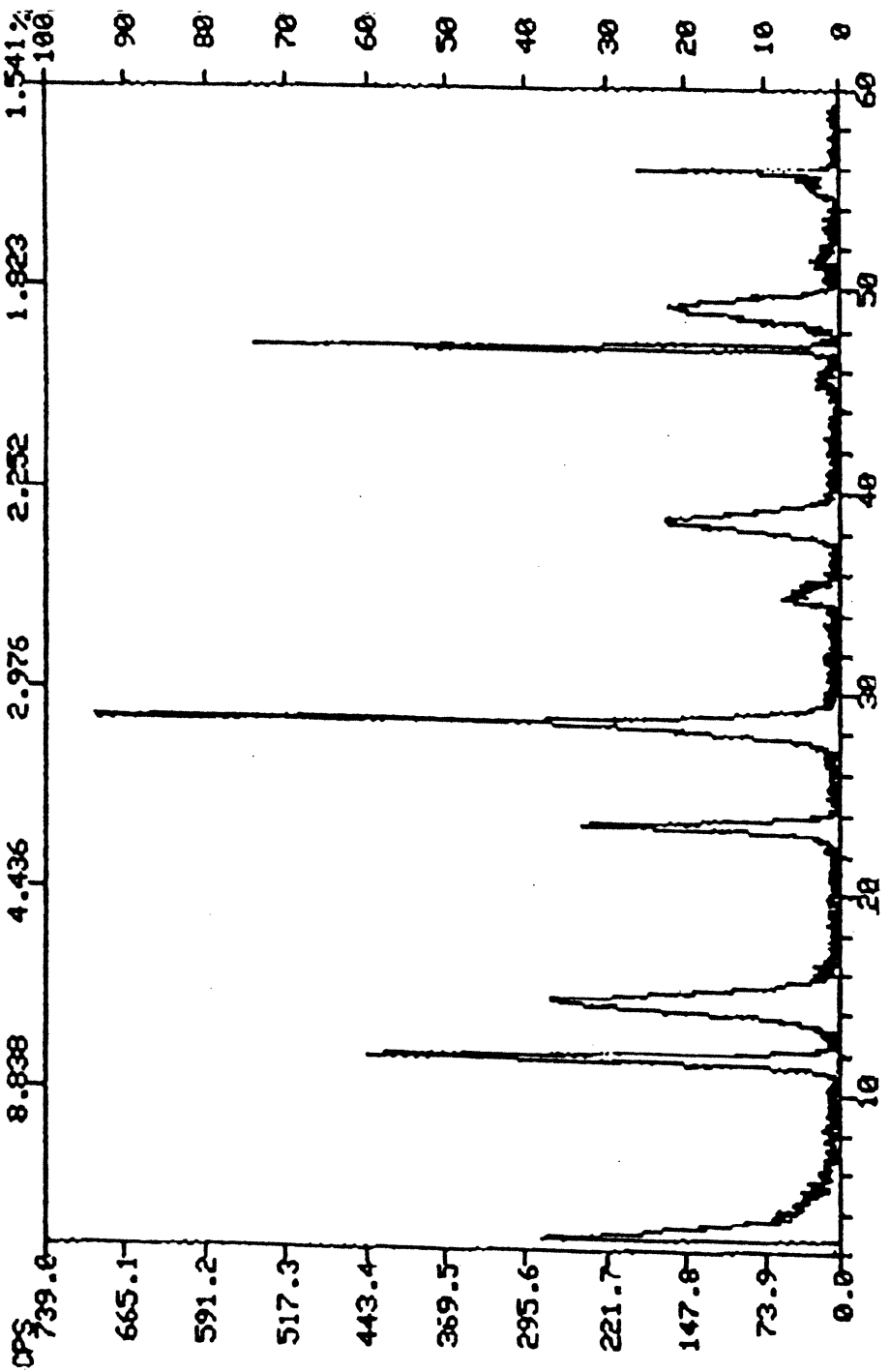

Fig 3.27 XRD trace of $Mg_2Al(OH)_6Cl$, directly synthesized in the presence of HCOH

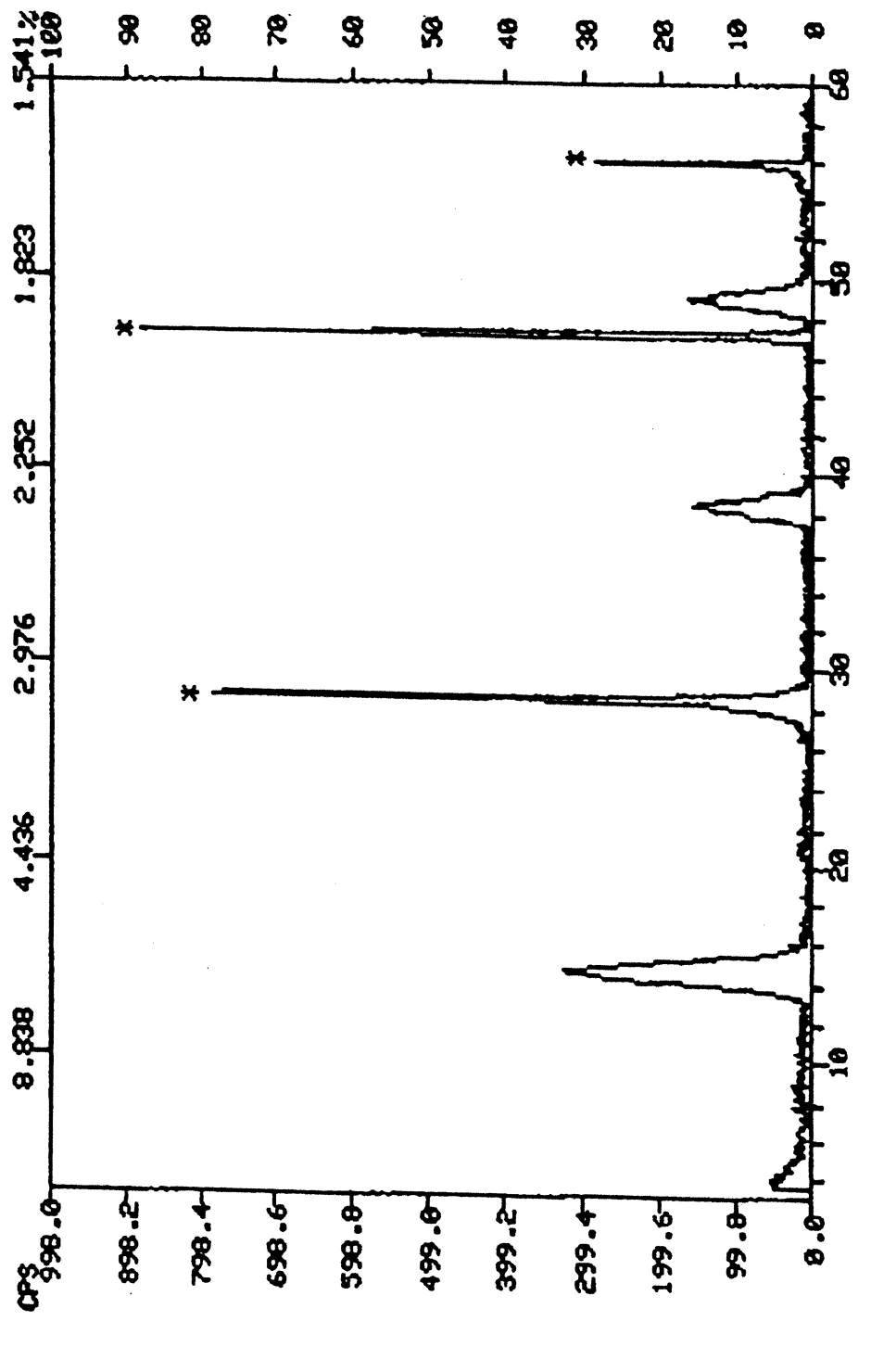

Fig 3.28 XRD trace of ethanolamine-containing LDH (* -- CaF_2 reference)

Table 3.12 XRD data of ethanolamine-containing LDH

2θ	best d (Å)	rel.int
14.594	6.055	37
28.524	3.123	(mixed with CaF_2)
38.284	2.357	22
49.125	1.870	31

ethanolamine. However, XRD patterns seems indicate something other than layered double hydroxide. Further work is needed.

3.3.4 Homogeneous Precipitation

It is well known that the morphology of precipitates is affected by the precipitation method employed. In the procedure of most of my work I mainly added (or titrated) NaOH solution directly to the reagent mixture. The precipitations in these cases were, actually, heterogeneous rather than homogeneous as there were always some kind of OH^- concentration distribution in the mixture. In other words pH in some regions could be very high while in other regions be quite low. Depending upon the rate of base addition and the effectiveness of stirring, the concentration of OH^- could vary significantly from region to region, causing different conditions for nucleation and growth of crystals.

To avoid such heterogeneous precipitation caused by imperfectness of mixing, a supposedly homogeneous method was employed. In this process, the precipitation was not carried out by adding OH^- but, rather, by decomposing some species which could yield OH^- ions directly or indirectly. In the following work urea and hexamine were used respectively to reveal the effectiveness by different precipitation methods.

3.3.4.1 Homogeneous Precipitation by Urea

Stoichiometric amounts of M^{2+} (M = Mg or Zn) and Al^{3+} were used in homogeneous precipitation. However, instead of NaOH, $(NH_2)_2CO$, which would be decomposed in heating to produce NH_4^+ and CO_3^{2-}, was used. The XRD results for $Zn_2Al(OH)_6(CO_3)_{1/2}$ and $Mg_2Al(OH)_6(CO_3)_{1/2}$ are depicted in Fig 3.29-3.30 and Table 3.13-3.14. Both of them display the XRD patterns for CO_3^{2-}-formed LDH as expected (2θ were around 11.47, 22.88 and 34.55), which indicated the success of homogeneous

Table 3.13 XRD data of $Zn_2Al(OH)_6(CO_3)_{1/2}$, from homogeneous precipitation by Urea

2θ	best d (Å)	rel.int
11.472	7.707	100
22.847	3.883	43
34.554	2.593	28
38.899	2.313	22

Table 3.14 XRD data of $Mg_2Al(OH)_6(CO_3)_{1/2}$, from homogeneous precipitation by Urea

2θ	best d (Å)	rel.int.
11.787	7.501	100
14.410	6.096	20
23.622	3.763	51
35.026	2.560	30
39.647	2.272	18
48.885	1.862	10

precipitation. In Fig 3.30 there are also some patterns for structures other than $Mg_2Al(OH)_6(CO_3)_{1/2}$, which might related to some other products produced in urea decomposition.

As mentioned above, the goal of homogeneous precipitation is improvement of crystal morphology. The pictures in Fig 3.31-3.32 revealed the SEM patterns for $Zn_2Al(OH)_6(CO_3)_{1/2}$ and $Mg_2Al(OH)_6(CO_3)_{1/2}$ precipitated by urea. Compared to $Zn_2Al(OH)_6(CO_3)_{1/2}$ obtained by heterogeneous precipitation, which were in irregular shapes (Fig 3.33), these samples were much better oriented. Particularly, in the case of $Zn_2Al(OH)_6(CO_3)_{1/2}$, SEM shows beautiful hexagonal morphology. These results indicated that homogeneous precipitation by urea could effectively improve LDHs crystallinity as expected.

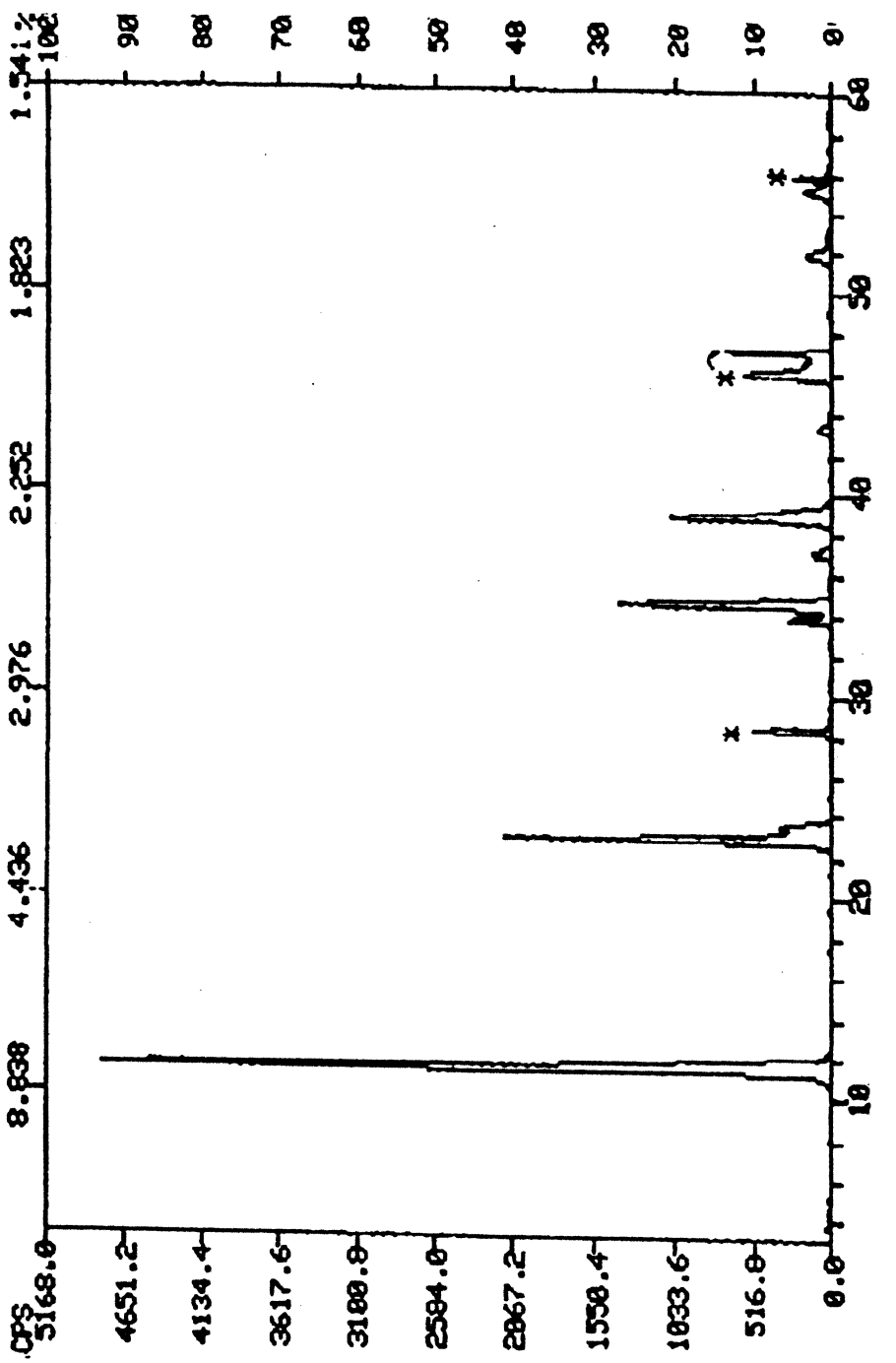

Fig 3.29 XRD trace of $Zn_2Al(OH)_6(CO_3)_{1/2}$, from homogeneous precipitation by Urea (* -- CaF_2 reference)

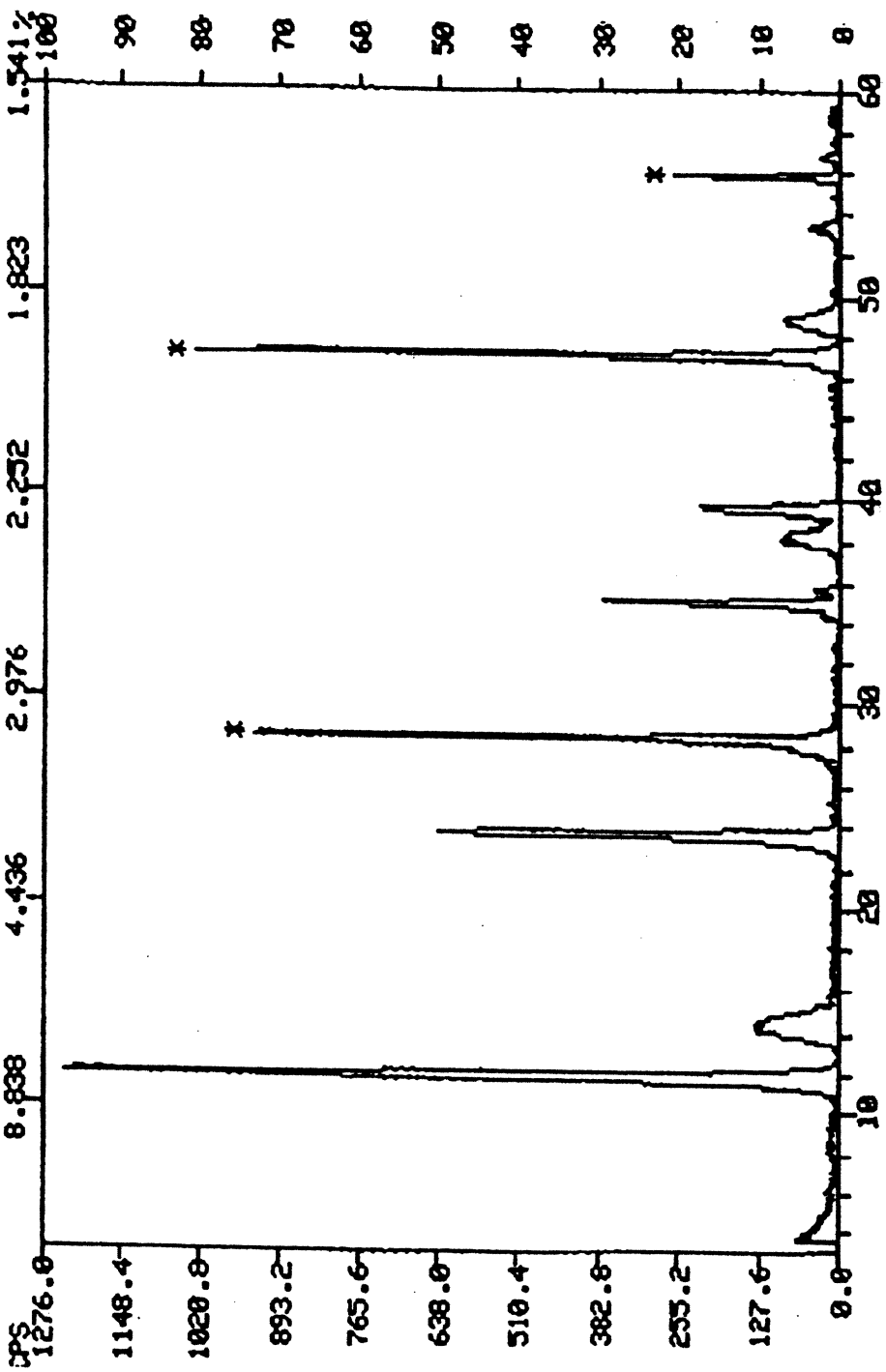

Fig 3.30 XRD trace of $Mg_2Al(OH)_6(CO_3)_{1/2}$, from homogeneous precipitation by Urea (* -- CaF_2)

3.3.4.2 Homogeneous Precipitation by Hexamine

Another reagent for homogeneous precipitation used in our work was hexamine. Different from urea cases, the decomposition of hexamine

$$N_4(CH_2)_6 + 6H_2O \longrightarrow 4NH_3 + 6CH_2O$$

base (NH_3) but does not provide needed anions. Thus NaCl (1.0 M) was introduced into the solution prior to precipitation. The procedures were quite similar to those employed in urea cases except that water had been degassed before using and the whole process was protected by nitrogen. The obtained solids were dried in a nitrogen flushed desiccator. The XRD traces and data in Fig 3.34-3.35 and Table 3.15-3.16 display the resulted $Zn_2Al(OH)_6Cl$ and $Mg_2Al(OH)_6Cl$ by hexamine respectively. Both figures reveal success of LDH formation. However,the SEM results shows no improved morphology; rather, the products were just aggregations of small irregular

Table 3.15 XRD data of $Zn_2Al(OH)_6Cl$, by hexamine precipitation

2θ	best d (Å)	rel.int.
11.525	7.672	100
23.061	3.854	55
34.622	2.588	11
39.039	2.305	12
46.309	1.959	11

Table 3.16 XRD data of $Mg_2Al(OH)_6Cl$, by hexamine precipitation

2θ	best d (Å)	rel.int.
11.506	7.685	100
23.062	3.854	50
34.020	2.589	17

particles. These results suggest that although hexamine could be used for homogeneous precipitation it might not improve particle crystallinity. The result might also imply that growing of Cl^--formed LDHs particles was not as easy as that of CO_3^{2-}-formed LDHs.

Fig 3.31 SEM of $Zn_2Al(OH)_6(CO_3)_{1/2}$, from homogeneous precipitation by urea

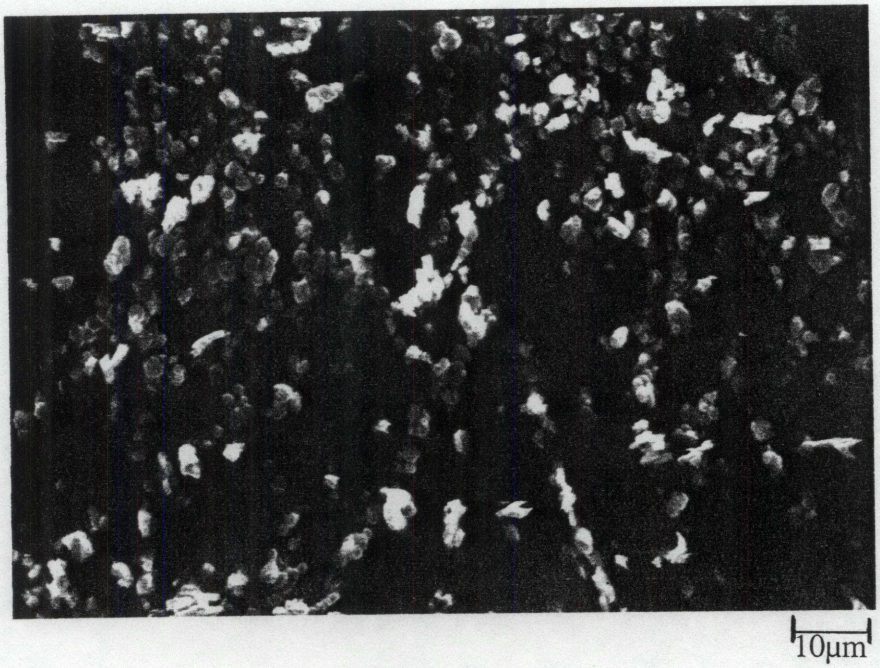

Fig 3.32 SEM of $Mg_2Al(OH)_6(CO_3)_{1/2}$, from homogeneous precipitation by urea

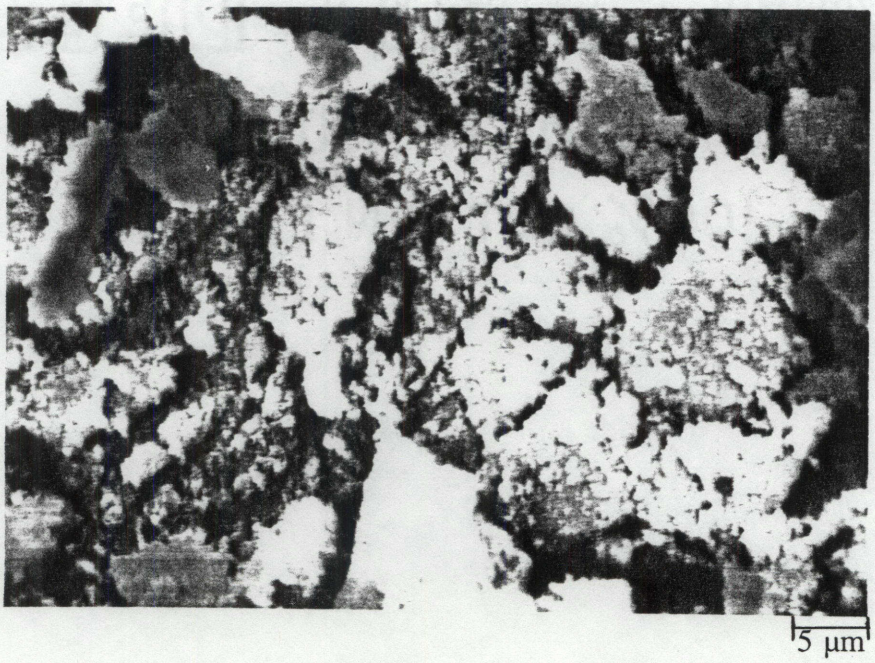

Fig 3.33 SEM of $Zn_2Al(OH)_6(CO_3)_{1/2}$, by "heterogeneous" precipitation

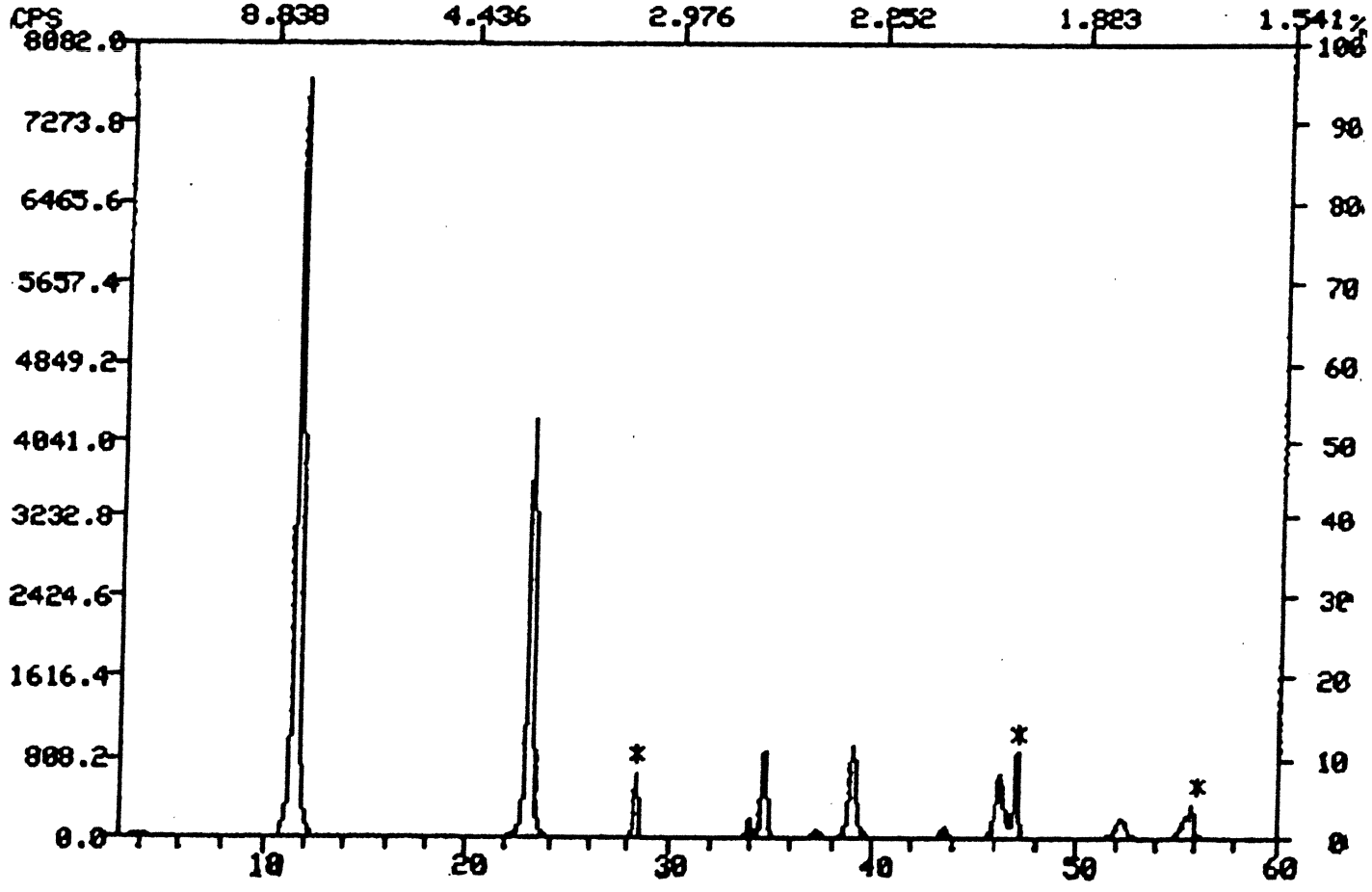

Fig 3.34 XRD trace of $Zn_2Al(OH)_6Cl$, by hexamine precipitation (* -- CaF_2 reference)

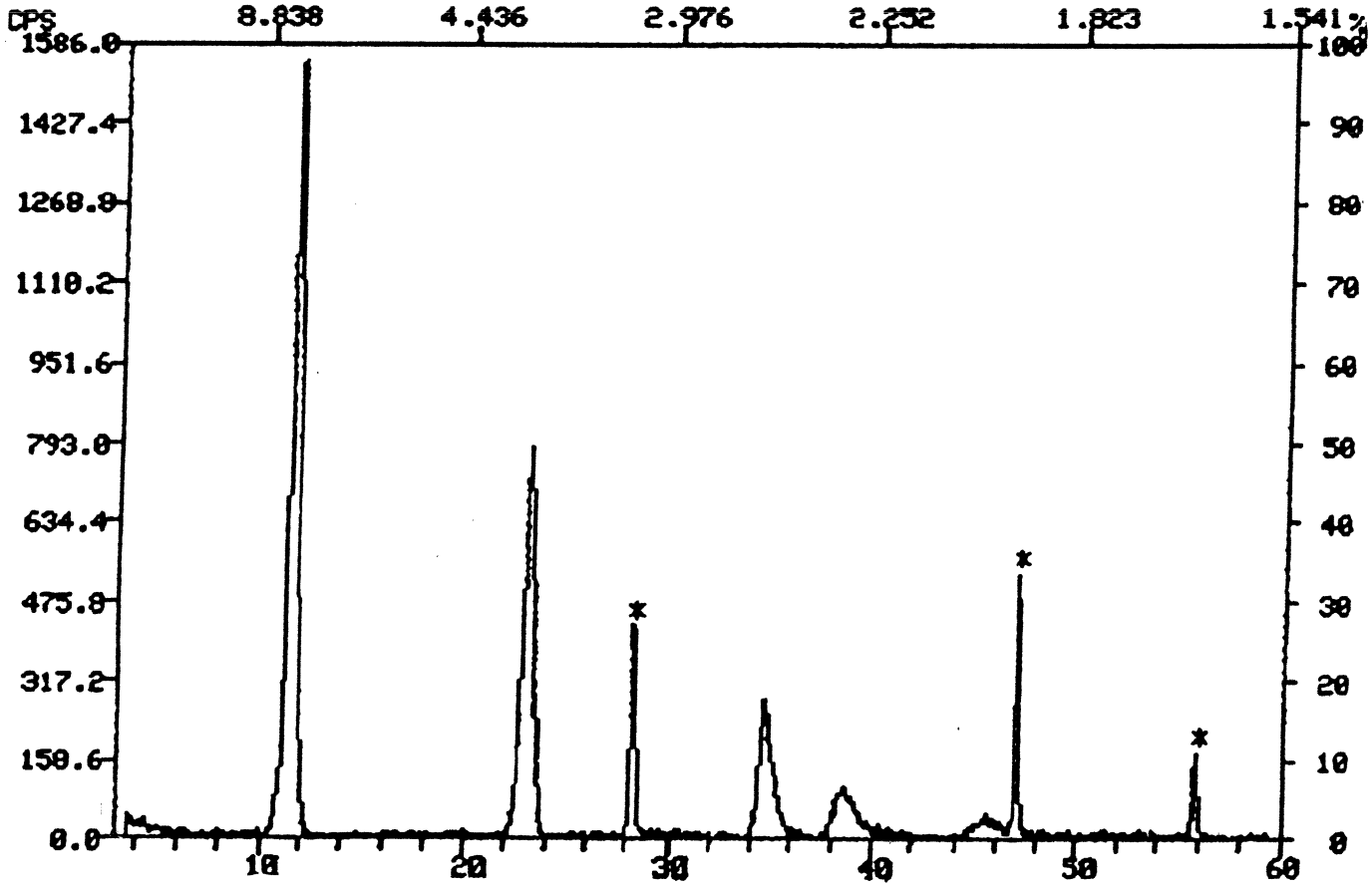

Fig 3.35 XRD trace of $Mg_2Al(OH)_6Cl$, by hexamine precipitation (* -- CaF_2 reference)

3.3.5 Effect of Thermo-agitation on Crystal forms

Nearly all of the samples in our works were agitated by refluxing precipitates overnight in order to grow crystal particle size. However, this process was not highly effective as none of the obtained samples shows well oriented morphology. One approach was to anneal a sample at 140°C, in a sealed bomb, for a week.

Fig 3.36 displays the SEM picture of $Mg_2Al(OH)_6Cl$ after annealing in its mother liquor. It shows increased crystal size as well as improved morphology. Obviously, the solid was well crystallized and oriented in slabs, which indicated the effectiveness of annealing under that condition. However, when part of the same sample was washed before annealing, it was still collection of fine irregular particles after annealing (Fig 3.37). This means that the environment of solids in annealing played an important role in the process. Possible relationships to the pH, ionic intensity, or Cl^- concentration in mother liquor were considered but have not yet been tested.

Another example was the annealing of $Mg_2Fe(OH)_6Cl$, which has already been discussed in section 3.3.2. We have seen, in that section, that the annealed $Mg_2Fe(OH)_6Cl$ sample became less vulnerable when exposed to S^{2-}, which could extract Fe^{3+} from iron-LDHs and destroy layered structures. This might be attributed to the growth of crystal particle size which, in turn, decreased the number of vulnerable irons by decreasing surface area.

Fig 3.36 SEM of $Mg_2Al(OH)_6Cl$, annealed at 140°C in mother liquor for 1 week

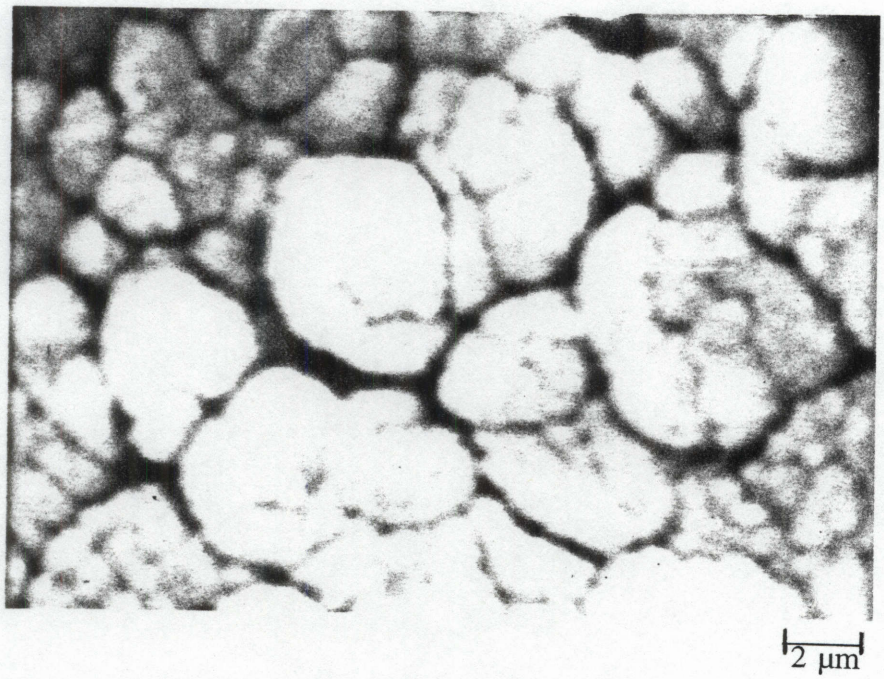

Fig 3.37 SEM of $Mg_2Al(OH)_6Cl$, annealed at 160°C, after washing, for 4 days

3.4 Conclusions and Suggestion for Further Studies

3.4.1 Conclusion

1. Ferrocyanide ions can be intercalated into LDHs in two ways: a) to replace the anion in the LDH framework and yield ferrocyanide-formed LDHs; b) to enter LDHs as a neutral molecule, which, in turn, could be transformed to LDH structural anion if the original anion is driven out by some physical means, such as heating.

2. SO_4-formed LDHs can be synthesized by either intercalation of SO_4^{2-} into LDHs or by oxidation of S-formed LDHs. The success of the latter technique also shows that S^{2-} can replace Cl^- in LDH. However, in that case if $Mg_2Fe(OH)_6Cl$ was used the iron LDH needed to be annealed before exchanging Cl^- with S^{2-} to reduce degradation of LDH structure, caused by S^{2-} attack on Fe^{3+} in the LDH framework.

3. It is possible to intercalate some simple organic species into LDH by means of exchange or direct synthesis. The included organic species can further be replaced by some other anions.

4. Homogeneous precipitation is, in some cases, a good approach to obtain better crystal morphology, in which nucleation of crystal would proceed homogeneously.

5. Annealing is another way to improve particle pattern, by which particles become larger in size and more oriented in shape. The effects of annealing depend on dissolved salts in liquid that require further exploration.

3.4.2 Suggestion for Further Studies

In above discussion (section 3.3.1) it has been suggested that ammonium ferrocyanide can enter LDHs as a neutral molecule. However, this species may in fact be some totally different material, such as $(NH_4)_4MgFe(CN)_6$ formed in layer decomposition. A way to test this is to synthesis these ascribed products and study and compare their FTIR and XRD data with the features described above.

There are also many questions that remained unsolved in our work. For example, in what form does an organic species exist in LDHs; what causes the difference when annealing is carried out in different environment; why an iron-formed LDH sulfide collapses in the oxidation by H_2O_2, etc. Besides, some basic methodology could also be worth of study, for instance, thermal treatment followed by intercalation of desired anions, which could lead to some expected LDH which can not be obtained by the usual method. It might also be interesting to expand the work into some application area. One of the topics would be potential use in liquid-solid heterogeneous catalysis which is less studied than gas-solid catalysis. According to the LDH's property, it has capacity to intercalate some species into its layers. Moreover, under appropriate conditions the inside species could diffuse out from LDH. This provides a possibility to develop some kind of catalysts which pick species from and release the products back to the solution. By the general formula introduced in chapter one, it is possible to substitute various divalent or trivalent metal cations, or to exchange potential anions with that in an existing LDH to obtain many different LDHs. Thus, it would be

reasonable to imagine to design and synthesize LDHs which have the ability to intercalate organic species and catalyze a desired reaction by interaction of those cations or anions with the entered species. Some potential catalytic active cations could be the transition metal in first or second period, such as Ni^{2+}, Co^{3+}, Cr^{3+}, Fe^{3+}, Fe^{2+}, Zn^{2+}, or even in main groups as Ga^{3+}, In^{3+} etc..

Another interesting area would be collection of materials from a solution. As LDHs are able to intercalate species from solution one potential application would be recovering valuable materials or removing harmful species from waste or recycle water. As those intercalation or exchanges are sometimes reversible it is possible that LDHs could be recycled. In this study, one of the interests would be the capacity of a designed LDH. Obviously, the higher the capacity the lower the cost. Thus, some studies would be focused on how to increase the capacity of a LDH; the relationship of capacity to the physical form (crystallinity) of an LDH. Another topic would be, for a specific LDH employed, to what extent a species could be removed form a solution. In other words, what is the lowest species concentration a LDH could remove form the solution, as this is quite important if a designed LDH could be used in waste water cleaning.

There are also many other topics which will widen the application of LDHs, such as those in electrochemical process. It is expected that studies will lead to increasing interest in this area.

REFERENCES

1. Socrates, G. Infrared Characteristic Group Frequencies, John Wiley & Sons Ltd: New York, **1980**, Chapter 10, 21.
2. Kendall, D. N. Applied Infrared Spectroscopy, Reinhold Publishing Corporation: London, **1966**, Chapter 17.
3. Nuttall, R. H., Sharp, D. W., and Waddington, T. C. J. Chem. Soc., **1960**, 4965.
4. Braterman, P. S. The Production, Concentration, and Arrangement of Prebiotic Materials by Inorganic Hosts, a proposal to NASA, **1993**.
5. Durig, J. R. Chemical, Biological and Industrial Application of Infrared Spectroscopy, John Wiley & Sons Ltd. **1985**, pp 111-128.
6. Sherwood, P. M. A. Vibrational Spectroscopy of Solids, Cambridge University Press, London, **1972**.
7. Farmer, V. C. The Infrared spectra of Mineral, Mineral Society, London, **1974**.
8. Szabo, I. N., Translated by Hedvig and H., Zentai G. Inorganic Crystal Chemistry, Akademiai Kiado, Budapest, **1969**, pp 333-343.
9. Kannan, S., Swamy, C. S. J. Mat. Sci. Lett, **1992**, 11, 1585-1587.
10. Taylor, R. M. Clays Clay Miner, **1980**, 15, 369.
11. Malki, K. E., Guanano, M., Forano, A., Roy, D., Besse, J. P. Mat. Sci. Forum, **1992**, 91-93, 171-176.
12. Miata, S., Kumura, T. Chem. Lett., **1973**, 834.

13. Meyn, M., Beneke, K., Lagaly, G. Inorg. Chem., **1990**, 29, 339.

14. Carrado, K. A., Forman, J. E., Botto, R. E., Winans, R. E. Chem. Mater., **1993**, 5, 472-478.

15. Nakamoto, K., Infrared and Raman Spectra of Inorganic and Coordinate Compounds, 4th Edition, **1986**, John Wiley & Sons Ltd.

16. Carrado, K. A., Kostapapas, A. Solid State Ionics, **1988**, 26, 77-86.

17. Constantino, V. R. L., Pinnavaia, T. J. Inorg. Chem., **1995**, 34, 883-892.

18. Malki, K. E., Roy, A. D., Basse, J. P. Mat. Res. Bull., **1993**, 28, 667-673.

17. McKenzie, A. I., Fisher, C. T., Davis, R. J. J. Cat., **1992**, 138, 547-561.

18. Dupuis, J., Battut, J. P., Fawal, Z., Hajjimohamad, H. Solid State Ionics, **1990**, 42, 251-255.

19. Shaw, B. R., Deng, Y. P., Strillacci, F. E., Carrado, K. A. J. Electrochem. Soc., **1990**, vol.137, pp 3136-3143.

20. Perezbernal, M. E., Ruanocasero, R., Pinnavaia, T. J. Cat. Lett., **1991**, vol.11, pp 55-62.

21. Ulibarri, M. A., Fernandaz, J. M., Labajos, F. M., Rives, V. Chem. Mat., **1991**, vol.3, pp 626-630.

22. Braterman, P. S., Tan, C., Zhao, J. Mat. Res. Bull., **1994**, Vol.29(12), pp 1217-1221.

REFERENCE LIST

Alzamora, L. E., Ross, J. R. H., Kruissink, E. C., Van Reijen. J. of Chem. Soc. Farad. Trans., **1981**, I 77, 665.

Bentley, F. F., Smithson, S. D., Rozek, A. L. Infrared Spectra and Characteristic Frequencies 700-300 cm^{-1}, Interscience Publishers, New York, **1968**.

Braterman, P. S. The Production, Concentration, and Arrangement of Prebiotic Materials by Inorganic Hosts, a proposal to NASA, **1993**.

Braterman, P. S., Tan, C., Zhao, J. Mat. Res. Bull., **1994**, Vol.29(12), pp 1217-1221.

Brindley, G. W., Kikkawa, S. Am. Mineral, **1979**, 64, 836.

Broers, A. N. SEM/1974, IIT research Institute: Chicago, **1974**.

Carrodo, K. A., Kostapapas, A. Solid State Ionics, **1988**, 26, 77-86.

Carrado, K. A., Forman, J. E., Botto, R. E., Winans, R. E. Chem. Mater., **1993**, 5, 472-478.

Chibwe, K., Jones, W. J. Chem. Soc. Chem. Comm., **1989**, 926-927.

Chibwe, K., Valim, J. B., Jones, W. Abstracts of papers of the American Chemical Society, **1989**, vol.198, 20.

Clark, R. J. H., Huster, R. E. in Spectroscopy of Inorganic-based Materials, Vol.14, John Wiley &. Sons, New York, **1987**.

Clearfield A., Kieke, M., Kwan, J., Colon, J. L., Wang, R. C. J. Inclusion Phenom. Mol. Recognit. Chem., **1991**, 11, 361.

Constantino, V. R. L., Pinnavaia, T. J. Inorg. Chem., **1995**, 34, 883-892.

Cullity, B. D., in Elements of X-ray Diffraction, Addison-Weiley ed., Massachusetts, **1987**, pp 284.

Dupuis, J., Battut, J, P., Fawal, Z., Hajjimohamad, H. Solid State ionics, **1990**, 42, 251-255.

Durig, J. R. in Chemical, Biological and Industrial Application of Infrared Spectroscopy, John Wiley &. Sons, New York, **1985**.

Farmer, V. C. The Infrared spectra of Mineral, Mineral Society, London, **1974**.

Farraro, J. R., Rein, A. J. in Fourier Transform Infrared Spectroscopy--Application to Chemical Systems, Ferraro, J. R., Basile, L. J., Eds., Academic Press: Orlando, Florida, **1985**, Vol.4, Chapter 6.

Fraser, D. J. J., Griffiths, P. R. Appl. Spectrosc, **1990**, 44(2), 193-199.

Fryer, J. R. The Chemical Application of Transmission Electron Microscopy, Academic Press: London, **1979**.

Grosso, R. P., Suib, S. L., Weber, R. S., Schubert, P. F. Chemistry of Material, **1992**, vol.4, 922-928.

Henning, O. in The Infrared Spectrum of Minerals, Farmer, V. C. Ed., Mineralogical Society: London, **1974**, Chapter 19.

Introduction to JSM-T 300 Scanning Microscope, JEOL LTD / JEOL Technics Ltd, Tokyo, Japan, **1980**.

Kandall, D. N. Applied Infrared Spectroscopy, Chapman &. Hall Ltd. London, **1966**.

Kannan, S., Swamy, C. S. J. Mat. Sci. Lett., **1992**, 11, 1585-1587.

Kokjiya, S. Sato, T., Nakayama, T., Yamashita, S., Makromol. Chem. Rapid Comm., **1981**, 2, 231.

Kruissink, E. C., Van Reijden, L. L. J. Chem. Soc. Farad. Trans., **1981**, I 77, 649.

Kwon, T., Tsigdinos, G. A., Pinnavaia, T. J. J. Am. Chem. Soc., **1988**, vol.10, 3653-3654.

Labajos, F. M., Rives, v., Ulibarri, M. A. Spectrosc. Lett., **1991**, vol.24, 499-508.

Lai, M., Howe, A. T. J. Chem. Soc. Chem. Comm., **1980**, 737.

Lai, M., Howe, A. T. J. solid state chem., **1981**, 39, 337.

Lee, Y. Thesis for Master Degree, Univ. North Texas, **1991**.

Leyden, D. E., Shreedhara Murthy, R. S. Spectroscopy, **1986**, 2, 28-36.

Lipson, H., Steeple, H. Interpretation of X-ray Powder diffraction Patterns, St. Martin's Press, New York, **1970**, pp 32.

Malki, K. E., Guonano, C., Forano, A., Roy, A. D., Besse, J. P. Mat. Sci. Forum, **1992**, Vol.91-93, 171-176.

Malki, K. E., Roy, A. D., Besse, J. P. Mat. Res. Bull., **1993**, Vol.28, 667-673.

Martin, K. J., Pinnavaia, T. J. J. Ame. Chem. Soc., **1986**, 61, 325.

Martin, K. J., Pinnavaia, T. J. J. Ame. Chem. Soc., **1986**, 108, 541-542.

McKenzie, A. I., Fisher, C. T., Davis, R. J. J. Cat., **1992**, 138, 547-561.

Meyn, M., Beneke, K., Lagaly, G. Inorg. Chem., **1990**, vol.29, 5201-5207.

Meyn, M., Beneke, K., Lagaly, G. Inorg. Chem., **1990**, 29, 339.

Miata, S. Clays Clay Miner, **1975**, 23, 369.

Miata, S., Kumura, T. Chem. Lett., **1973**, 834.

Miyata, S., Hirose, T. Clays Clay Miner, **1978**, 26, 441.

Mollah, M. Y. A., Tsai, Y. N., Hess, T. R., Cocke, D. L. J. Hazardous Materials, **1992**, 30(3), 273-283.

Nakamoto, K., Infrared and Raman Spectra of Inorganic and Coordinate Compounds, 4th Edition, **1986**, John Wiley & Sons Ltd.

Nakatsuka, H., Kawasaki, S., Yamashita, S., Kokjiya, S. Bull. Chem. Soc. Japan, **1979**, 52, 244a.

Narita, E., Kaviratna, P., Pinnavaia, T. J. Chem. Lett., **1991**, 5, 805-808.

Narita, E., Yamagishi, T., Tonai, T. Nippon Kagaku Kaishi, **1992**, 3, 291-296.

Narita, E., Yamagishi, T., Suzuki, K. Nippon Kagaku Kaishi, **1992**, 6, 676-679.

Nuttall, R. H., Sharp, D. W., and Waddington, T. C. J. Chem. Soc., **1960**, 4965.

Ortego, J. D., Jackson, S., Yu, G., McWhinney, H., Cocke, D. L. J. Environ. Sci. Health, **1989**, A24(6).

Park, I. Y. J. Chem. Soc. Dolton, **1990**, 3071.

Perezbernal M. E., Ruanocasero, R., Pinnavaia, T. J. Cat. Lett., **1991**, vol.11, 55-62.

Pinnavaia, T. J., Rameswaran, M., Dimotakis, E. D., Giannelis, E. P., Rightor, E. G. Faraday Discussions of the Chemical Society, **1989**, 87, 227-237.

Powder Diffraction file-Inorganic phases, International Center for Diffraction Data:

Swartmore. PA. **1983**.

Rameswaran, M., Pinnavaia, T. J., Abstracts of Papers of the American Chemical Society, **1988**, 196, 55.

Reichle, W. T. J. Cat., **1985**, 94, 547.

Reichle, W. T. Solid State Ionics, **1986**, 22, 135.

Robbins, E. I., Iberall, Geomicrobiology Journal, **1991**, vol.9, 51-66.

Sakurai, T., Sato, T., Yoshinaga, A. Proc. 5th Int. Symp. Chem. Cem., Tokyo, **1968**, Vol.1, pp 300-321.

Schollhorn, R., Otto, B. J. Chem. Soc. Chem. Comm., **1986**, 1222.

Shaw, B. R., Deng, Y. P., Strillacci, F. E., Carrado, K. A., Fessehaie, M. G. J. Electrochem. Soc., **1990**, vol.137, 3136-3143.

Sherwood, P. M. A. Vibrational Spectroscopy of Solids, Cambridge University Press, London, **1972**.

Skoog, D. A. Principle of Instrumental Analysis, 3rd ed., Saunders College: Philadelphia, **1985**, pp 257-258.

Socrates, G. Infrared Characteristic Group Frequencies, John Wiley & Sons Ltd: New York, **1980**, Chapter 10, 21.

Szabo, I. N., Translated by Hedvig and H., Zentai G. Inorganic Crystal Chemistry, Akademiai Kiado, Budapest, **1969**, pp 333-343.

Taylor, R. M. Clays Clay Miner, **1980**, 15, 369.

Ulibarri, M. A., Fernandaz, J. M., Labajos, F. M., Rives, V. Chem. Mat., **1991**,

vol.3, pp 626-630.

Van Every, K. W., Griffiths, P. R. Appl. Spectrosc., **1991**, 45(3), 347-359.

Wang, J. D., Tian, Y., Clearfield, A. Abstracts of papers of the American Chemical Society, **1992**, vol.203, 785.

Zhao, B. PhD Dissertation, University of North Texas, **1993.**